CIN85 modulates TGFβ signaling by promoting the presentation of TGFβ receptors on the cell surface

Ihor Yakymovych,[1] Mariya Yakymovych,[1] Guangxiang Zang,[2] Yabing Mu,[2] Anders Bergh,[2] Maréne Landström,[1,2]* and Carl-Henrik Heldin[1]*

[1]Science for Life Laboratory, Ludwig Institute for Cancer Research Ltd., Uppsala University, SE-75124 Uppsala, Sweden
[2]Department of Medical Biosciences and Pathology, Umeå University, SE-90185 Umeå, Sweden

Members of the transforming growth factor β (TGFβ) family initiate cellular responses by binding to TGFβ receptor type II (TβRII) and type I (TβRI) serine/threonine kinases, whereby Smad2 and Smad3 are phosphorylated and activated, promoting their association with Smad4. We report here that TβRI interacts with the SH3 domains of the adaptor protein CIN85 in response to TGFβ stimulation in a TRAF6-dependent manner. Small interfering RNA–mediated knockdown of CIN85 resulted in accumulation of TβRI in intracellular compartments and diminished TGFβ-stimulated Smad2 phosphorylation. Overexpression of CIN85 instead increased the amount of TβRI at the cell surface. This effect was inhibited by a dominant-negative mutant of Rab11, suggesting that CIN85 promoted recycling of TGFβ receptors. CIN85 enhanced TGFβ-stimulated Smad2 phosphorylation, transcriptional responses, and cell migration. CIN85 expression correlated with the degree of malignancy of prostate cancers. Collectively, our results reveal that CIN85 promotes recycling of TGFβ receptors and thereby positively regulates TGFβ signaling.

Introduction

Members of the TGFβ family of multifunctional cytokines govern key cellular functions via binding to transmembrane serine/threonine kinases named TGFβ receptor type I (TβRI) and type II (TβRII; Heldin and Moustakas, 2012; Xu et al., 2012). Ligand binding initiates signaling by activation of the Smad family of transcription factors, which are central mediators of TGFβ signaling to the nucleus. In addition, TGFβ receptors activate non-Smad signaling pathways, such as extracellular signal-regulated kinase p38 and JNK MAPKs, AKT (Mu et al., 2012), and the small GTPases Rho, Rac, and Cdc42 (Kardassis et al., 2009). The initiation and regulation of TGFβ signaling is achieved by posttranslational modifications of signaling components, which determine the subcellular localization, activity, and duration of the signal. Several receptor-interacting proteins, such as Smad7, ELF, and SARA, play critical roles in the proper control of Smad access to the receptors (Mishra and Marshall, 2006). The ubiquitin ligase tumor necrosis factor receptor-associated factor 6 (TRAF6) mediates activation of p38 and JNK by TGFβ (Sorrentino et al., 2008; Yamashita et al., 2008). Other receptor-associated proteins, such as cPML and Dab2, have roles in vesicular trafficking of the receptors (Lin et al., 2004; Penheiter et al., 2010).

CIN85 (Cbl-interacting protein of 85 kD, also called SH3 domain kinase binding protein 1 [SH3KBP1]) is a ubiquitously expressed adaptor protein that has been shown to associate with several signaling proteins, thus linking it to many cellular compartments and processes, including signal transduction, vesicle-mediated transport, cytoskeleton remodeling, programmed cell death, and viral infection (Dikic, 2002; Kowanetz et al., 2004; Havrylov et al., 2010). The N terminus of CIN85 is composed of three SH3 domains that mediate interactions with various proteins, typically containing proline-rich sequences (Dikic, 2002). It was also demonstrated that all three SH3 domains bind ubiquitin (Bezsonova et al., 2008). The proline-rich region of CIN85, localized between SH3 domains and the C terminus, is a recognition site for other SH3 domain–containing proteins, such as the p85 subunit of phosphatidylinositol-3′-kinase (Gout et al., 2000), kinases of Src family (Dikic, 2002), p130Cas, and cortactin (Lynch et al., 2003). The C-terminal coiled-coil region of CIN85 mediates its dimerization (Watanabe et al., 2000) and binds to phosphatidic acid on cell membranes (Zhang et al., 2009). CIN85 has been implicated in the control of internalization of receptor tyrosine kinases (Szymkiewicz et al., 2004), including the receptors for EGF (Soubeyran et al., 2002), hepatocyte growth factor (Petrelli et al., 2002), platelet-derived growth factor, and stem cell factor (Szymkiewicz et al., 2002), as well as the dopamine receptor (Shimokawa et al., 2010). Besides, CIN85 participates in post-endocytic EGF receptor (EGFR) trafficking and degradation (Schroeder et al., 2010,

*M. Landström and C.-H. Heldin contributed equally to this paper.

Correspondence to Carl-Henrik Heldin: c-h.heldin@licr.uu.se

Abbreviations used in this paper: EGFR, EGF receptor; HEK, human embryonic kidney; qRT-PCR, quantitative RT-PCR; TβRI, TGFβ receptor type I; TRAF6, tumor necrosis factor receptor-associated factor 6.

The Rockefeller University Press $30.00
J. Cell Biol. Vol. 210 No. 2 319–332
www.jcb.org/cgi/doi/10.1083/jcb.201411025

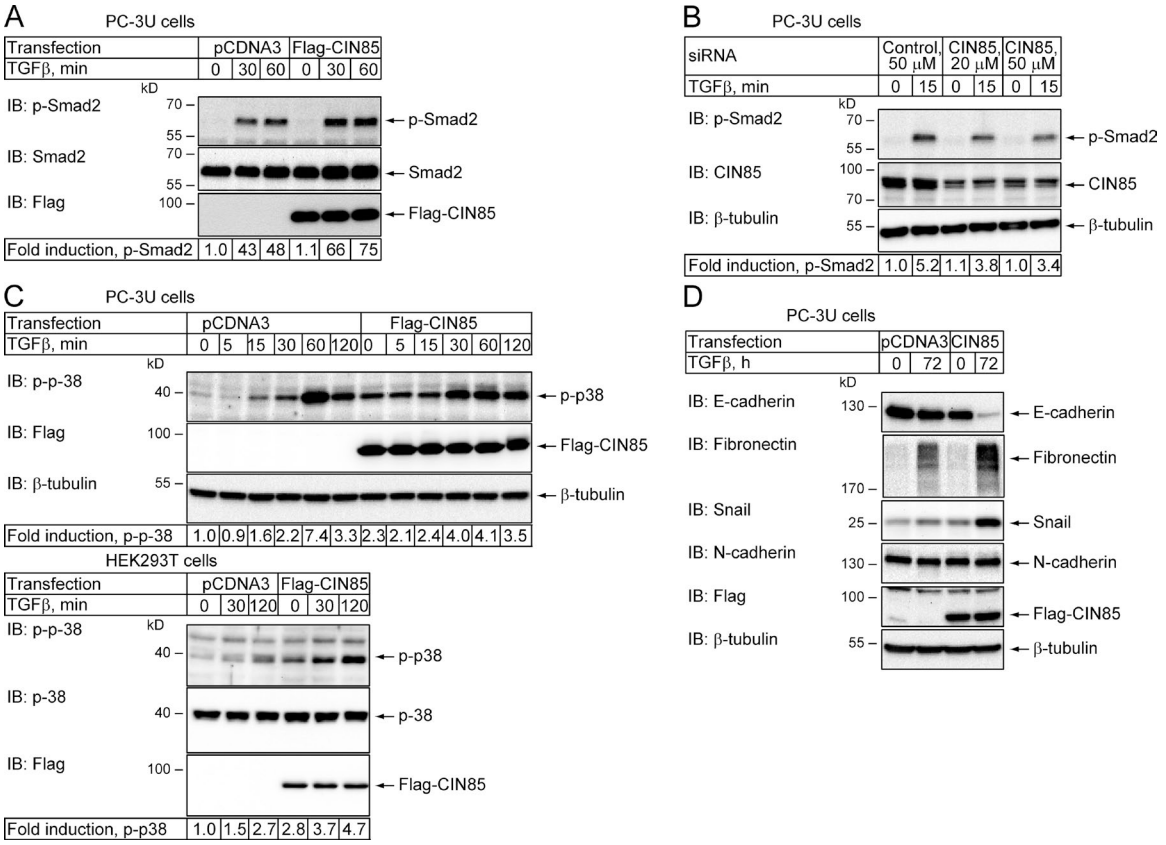

Figure 1. **CIN85 enhances TGFβ signaling.** (A) PC-3U cells were transfected with empty vector (pCDNA3) or Flag-CIN85 plasmid and stimulated with 5 ng/ml TGFβ, as indicated. Cell lysates were prepared and the levels of phosphorylated Smad2, total Smad2, and Flag-CIN85 were analyzed by immunoblotting. (B) PC-3U cells were transfected with control siRNA or different amounts of CIN85-siRNA and incubated with 5 ng/ml TGFβ for 15 min, as indicated. Cell lysates were prepared and the level of phosphorylated Smad2 and the efficiency of CIN85 knockdown were analyzed by immunoblotting. The membrane was stripped and probed for tubulin to confirm equal loading. (C) PC-3U cells (top) or HEK293T cells (bottom) were transfected with control plasmid or Flag-CIN85 and stimulated with 5 ng/ml TGFβ, for the indicated time periods. Cell lysates were prepared and the level of phosphorylated p38 MAPK was analyzed by immunoblotting. The efficiency of transfection was evaluated by blotting with Flag antibodies and loading was assessed by probing for tubulin. (D) PC-3U cells were transfected with control or Flag-CIN85 plasmids. At 48 h after transfection, TGFβ (5 ng/ml) was added to the culture media for an additional 72 h. The expression of E-cadherin, N-cadherin, fibronectin, and Snail was analyzed by immunoblotting. The efficiency of transfection was evaluated by incubation of the membrane with Flag antibodies and loading was determined by probing for tubulin.

2012; Rønning et al., 2011). In addition to affecting endocytosis and trafficking of transmembrane proteins, CIN85 has been reported to control the level of the nonreceptor tyrosine kinase Syk (Peruzzi et al., 2007) and to link B cell receptor signaling to the canonical NF-κB pathway (Kometani et al., 2011).

In this study, we have investigated the role of CIN85 in the regulation of TGFβ signaling. We found that CIN85 enhances TGFβ-induced signaling and cellular responses to TGFβ by promoting the expression of TGFβ receptors on the surface in a Rab11-dependent manner. We have also shown that CIN85 interacts with TβRI in a TRAF6-dependent manner.

Results

CIN85 augments TGFβ-induced intracellular signaling events, activation of transcription, and cell motility

As CIN85 has been shown to interact with many components of signaling pathways affected by TGFβ, we investigated its effect on TGFβ signaling. We found that TGFβ treatment caused ∼1.5 times stronger phosphorylation of Smad2 in PC-3U cells overexpressing CIN85 than in control cells (Fig. 1 A). Moreover, down-regulation of CIN85 by siRNA transfection reduced TGFβ-dependent Smad2 phosphorylation (Fig. 1 B). TGFβ-induced phosphorylation of p38 MAPK was also enhanced by CIN85 overexpression in human embryonic kidney (HEK) 293T and PC-3U cells (Fig. 1 C). However, because the background phosphorylation of p38 was enhanced about twofold in CIN85 overexpressing cells, the fold increase after TGFβ stimulation was less affected. It is possible that overexpression of CIN85 makes cells more sensitive to endogenously synthesized TGFβ, or CIN85 may activate p38 through other mechanisms that are not directly connected to TGFβ signaling (Aissouni et al., 2005; Kim et al., 2013).

In addition, other known effects of TGFβ on the protein expression in cells were also strengthened by CIN85. Thus, in PC-3U cells the TGFβ-induced expression of fibronectin and Snail, and the down-regulation of E-cadherin, were enhanced in cells overexpressing CIN85 compared with untransfected cells (Fig. 1 D). N-Cadherin expression in PC-3U cells was not affected by TGFβ treatment or by CIN85 overexpression (Fig. 1 D).

To further investigate the role of CIN85 in TGFβ signaling, we performed Smad-specific promoter reporter assays. In agreement with the aforementioned results, transfection of HEK293T and PC-3U cells with increasing amounts of CIN85

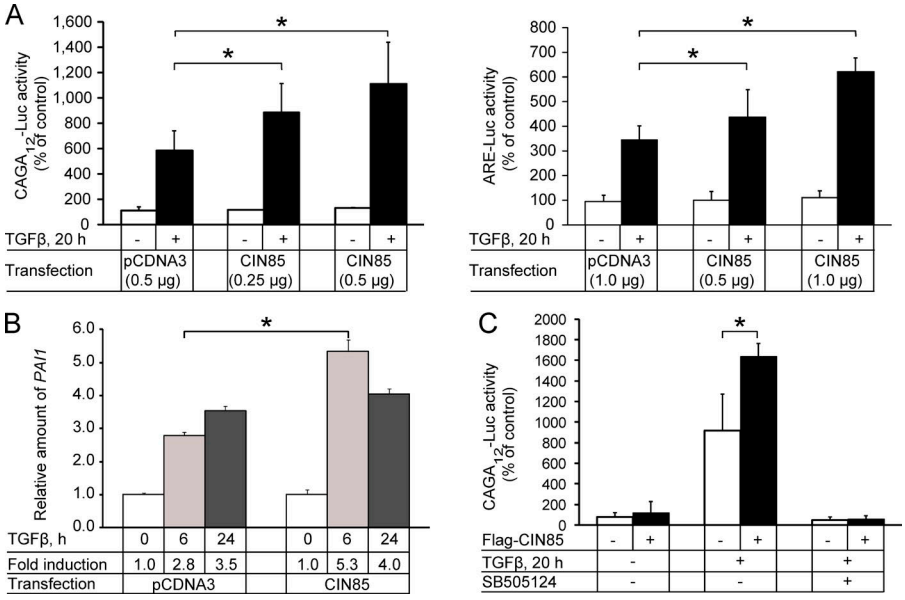

Figure 2. **CIN85 enhances TGFβ transcriptional activity.** (A) HEK293T cells, transfected with $CAGA_{12}$-Luc (left) or xFAST/ARE-Luc (right) and different amounts of Flag-CIN85 plasmid, were not treated (open bars) or treated with 5 ng/ml TGFβ (shaded bars) for 20 h, and luciferase activity was measured. The results are presented as the mean (in percentage of control) of six independent experiments. Error bars represent SD. (B) qRT-PCR analysis for expression for PAI-1 was performed on mRNA extracted from PC-3U cells transiently transfected with empty pCDNA3 vector or Flag-CIN85 and treated with 5 ng/ml TGFβ for the indicated time periods. The results were normalized on the basis of GAPDH mRNA expression. The data are plotted as the mean fold induction of TGFβ-stimulated mRNA levels relative to unstimulated levels (0 h set to 1) with SD determined from triplicate measurements. Results of one representative experiment out of three performed are shown. (C) HEK293T cells transfected with $CAGA_{12}$-Luc reporter and control plasmid (open bars) or Flag-CIN85 plasmid (shaded bars). The cells were pretreated for 1 h with DMSO or TβRI kinase inhibitor SB505124 (10 μM) and then incubated with 5 ng/ml TGFβ for 20 h as indicated. Luciferase activity was measured and transfection efficiency was normalized to β-galactosidase activity. The results are presented as the mean (in percentage of control) of three independent experiments. Error bars represent SD. *, $P < 0.05$ cells transfected with CIN85 compared with cells transfected with empty vector.

enhanced TGFβ-dependent activation of $CAGA_{12}$-Luc and ARE-Luc reporters in a dose-dependent manner (Fig. 2 A). The level of endogenous PAI-1 mRNA was also higher in PC-3U cells overexpressing CIN85 after treatment with TGFβ (Fig. 2 B). The effect of CIN85 on TGFβ-induced activation of transcription was dependent on the receptor kinase activity; treatment of the cells with a specific inhibitor of the TβRI kinase (SB505124) completely blocked activation of the $CAGA_{12}$-Luc reporter in control cells as well as in the cells overexpressing CIN85 (Fig. 2 C).

Additionally, CIN85 enhanced TGFβ-induced migration of PC-3U cells. In a tissue culture wound-healing assay PC-3U cells overexpressing CIN85 closed the wound faster in response to TGFβ stimulation compared with control cells (Fig. 3). These observations further support the conclusion that CIN85 enhances TGFβ signaling.

CIN85 interacts physically with TGFβ receptors

To explore the mechanisms for CIN85-mediated enhancement of TGFβ signaling, we investigated whether CIN85 binds to TGFβ receptors. Lysate of HEK293T cells overexpressing Flag-CIN85 and HA-TβRI was subjected to immunoprecipitation using an HA antibody, followed by immunoblotting using a Flag antibody. A band with the expected size of Flag-CIN85 was seen in the lane corresponding to a lysate of cells stimulated with TGFβ, but not in the lane corresponding to unstimulated cells (Fig. 4 A), suggesting that TβRI and CIN85 make a complex after ligand treatment. Endogenous CIN85 and TβRI were also reciprocally coimmunoprecipitated from lysates of PC-3U cells by antibodies against TβRI and CIN85, respectively, in a TGFβ-dependent manner (Fig. 4 B). CIN85 was also coimmunoprecipitated with TβRII; however, in this case interaction did not depend on the treatment of cells with TGFβ (Fig. 4 C). These results suggest that both TGFβ receptors can form a complex with CIN85 and that interaction between TβRI and CIN85 is enhanced by ligand treatment.

We explored if the kinase activities of the TGFβ receptors are important for the interaction between TβRI and CIN85. We pretreated the HEK293T cells, transfected or not by CIN85, with an inhibitor of the TβRI kinase (SB505124) or with an inhibitor of both TβRI and TβRII kinases (LY2109761), and immunoprecipitated TβRI from the lysates of these cells. TGFβ enhanced the interaction between TβRI and CIN85, but the kinase inhibitors had no effect on the amount of CIN85 coprecipitated with TβRI (Fig. S1 A). In addition, inhibition of internalization by low temperature or by the dynamin inhibitor dynasore did not prevent TGFβ-induced TβRI interaction with CIN85 (Fig. S1, B and C). These results suggest that neither the kinase activities of the receptors nor endosomal trafficking are needed for ligand-enhanced TβRI binding to CIN85.

CIN85 consists of three SH3 domains in the N-terminal half of the molecule and a proline-rich region and coiled-coil domain in the C terminus (Fig. 4 D). Coimmunoprecipitation experiments revealed that a deletion mutant of CIN85 that contained three SH3 domains coprecipitated with TβRI, whereas a mutant that encompassed the proline-rich and coiled-coil domains did not (Fig. 4 E). Similarly, only full-length CIN85 and the SH3 domains containing deletion mutant, but not the deletion mutant that contained only the C-terminal part, were coprecipitated with HA-TβRII (Fig. 4 F). To further delineate which part of CIN85 is critical for the interaction with TβRI, we performed GST pull-down assays. Consistent with the results of coimmunoprecipitation experiments (Fig. 4 E), only the N-terminal part of CIN85 was found to interact with TβRI (Fig. S2 A). GST fusion proteins that consisted of only the SH3-A or only the SH3-B domain of CIN85 both interacted with TβRI, but less efficiently than the GST fusion construct that included all three SH3 domains of CIN85 (Fig. S2 A). The N-terminal part of CIN85 was less efficient in enhancing TGFβ-induced ac-

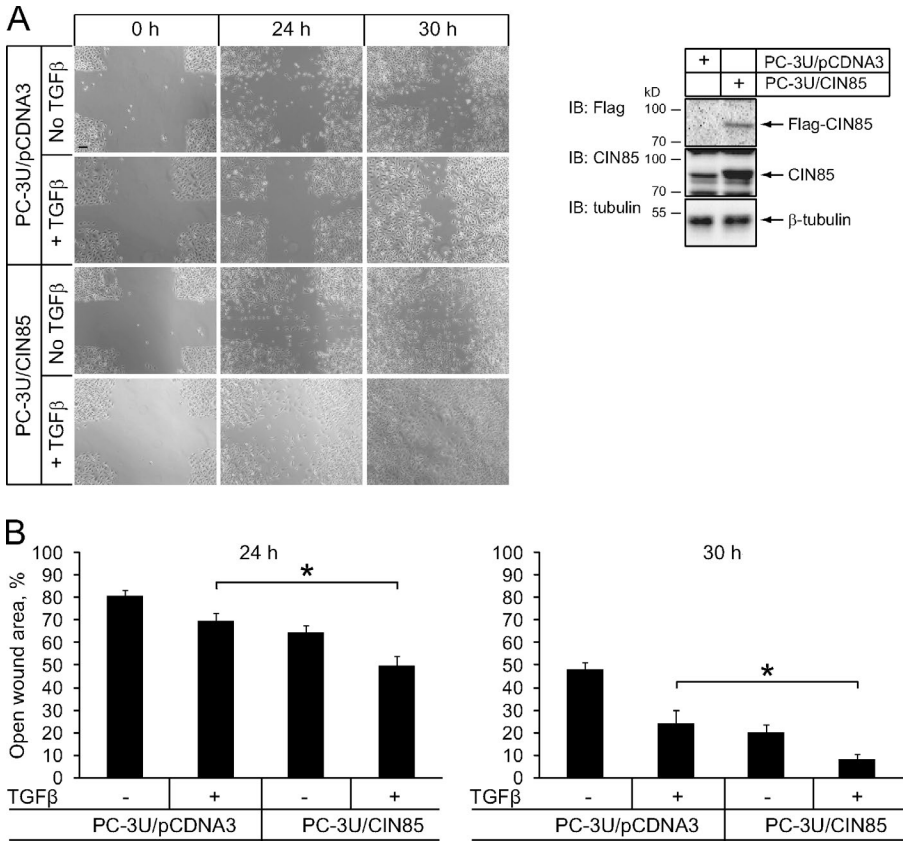

Figure 3. **CIN85 enhances TGFβ-induced cell migration.** (A) PC-3U cells were transfected with either an empty pcDNA3 vector or a Flag-CIN85 expression construct. To increase the percentage of transfected cells, they were cultured in medium with 0.4 mg/ml G418 for 10 d. Expression of Flag-CIN85 in the cells was evaluated by blotting with Flag and CIN85 antibodies (right). For the in vitro wound healing assay, cells were grown to confluence in 6-well plates and TGFβ (5 ng/ml) was added to culture medium supplemented with 0.1% FBS immediately after wounding. Phase-contrast images were captured after 24 and 30 h. Representative images for control (PC-3U/pCDNA3) and Flag-CIN85 expressing (PC-3U/CIN85) cells at different time points are shown (left). Bar, 200 µm. (B) Quantification of the motility of PC-3U/pCDNA3 and PC-3U/CIN85 cells in the cell culture wound healing assay was performed on 12 measurements in each experimental condition and expressed as a percentage of the open wound area. Data represent means ± SD. Brackets indicate the comparisons that showed significant differences in migration of control cells and cells overexpressing CIN85 under TGFβ treatment. Three independent experiments were done. *, $P < 0.05$.

tivation of the $CAGA_{12}$ luciferase reporter, when compared with full-length CIN85 (Fig. 4 G), suggesting that the proline-rich and/or coiled-coil domains are also important for the enhancement of TGFβ signaling by CIN85.

To explore whether CIN85 and TβRI coexist in the same intracellular compartments, we performed immunofluorescence staining of COS7 cells expressing both proteins. Colocalization of CIN85 with TβRI was detected in the perinuclear region, intracellular vesicles, and membrane ruffles (Fig. 4 H). Quantitation of the immunostained images suggested that 14 ± 3% of the TβRI were colocalized with CIN85 at the cell periphery; this number did not change in cells treated with TGFβ, suggesting that the distribution of either of the proteins was not affected by TGFβ treatment. In contrast, the increased coimmunoprecipitation of TβRI and CIN85 in lysates from cells treated with TGFβ (Fig. 4, A and B) suggests that ligand stimulation somehow modifies TβRI and/or CIN85 in a manner that enhances the affinity of the proteins for each other.

TRAF6 ubiquitinates CIN85 and enhances its binding to TβRI

Next, we studied possible means by which TGFβ stimulation promotes the interaction between TβRI and CIN85. Because all three SH3 domains of CIN85 bind to ubiquitin (Bezsonova et al., 2008) and TGFβ stimulation, via the E3 ubiquitin ligase TRAF6, causes polyubiquitination of TβRI (Mu et al., 2011; Sundar et al., 2015), we investigated whether TRAF6 plays a role in the interaction between CIN85 and TβRI. We found that TGFβ stimulation of HEK293T cells overexpressing CIN85 and TRAF6 induced ubiquitination of CIN85 (Fig. 5 A). Moreover, inhibition of TRAF6 expression by siRNA decreased ubiquitination of CIN85 in cells treated with TGFβ (Fig. 5 B).

To explore further the effect of TRAF6 on TβRI–CIN85 complex formation, HA-TβRI was immunoprecipitated from the lysates of HEK293T cells transfected with Flag-CIN85 and HA-TβRI, in the presence or absence of Flag-TRAF6. The TGFβ-induced coprecipitation of TβRI and CIN85 was enhanced upon coexpression of TRAF6 in the cells (Fig. 5 C). In contrast, TGFβ treatment did not affect coimmunoprecipitation of CIN85 with mutant TβRI(E161A), which is unable bind to TRAF6 (Sorrentino et al., 2008; Fig. 5 D). Moreover, treatment of TRAF6-deficient mouse embryonic fibroblasts with TGFβ did not enhance coimmunoprecipitation of endogenous CIN85, whereas a coimmunoprecipitation was seen in wild-type mouse embryonic fibroblasts (Fig. 5 E). The interaction of TβRII with CIN85 was not affected by overexpression of TRAF6, with or without stimulation with TGFβ (Fig. S2 C).

To elucidate the importance of the enzymatic activity of TRAF6 for the CIN85–TβRI interaction, we used a ligase-inactive mutant of TRAF6 in the coimmunoprecipitation experiments. In contrast to wild-type TRAF6, mutant TRAF6 was unable to promote the interaction between the receptor and CIN85 (Fig. 5 C). Moreover, GST-TβRI ubiquitinated by TRAF6 in vitro precipitated CIN85 more efficiently than nonubiquitinated GST-TβRI (Fig. S2 B). Thus, our observations support the notion that the enzymatic activity of TRAF6 is important for TGFβ-induced interaction between TβRI and CIN85.

CIN85 regulates the intracellular localization of TβRs

Similar to many other adaptor proteins, CIN85 has been reported to take part in multiple cellular processes including internalization of several activated receptor tyrosine kinases and their vesicle-mediated transport (Szymkiewicz et al., 2004;

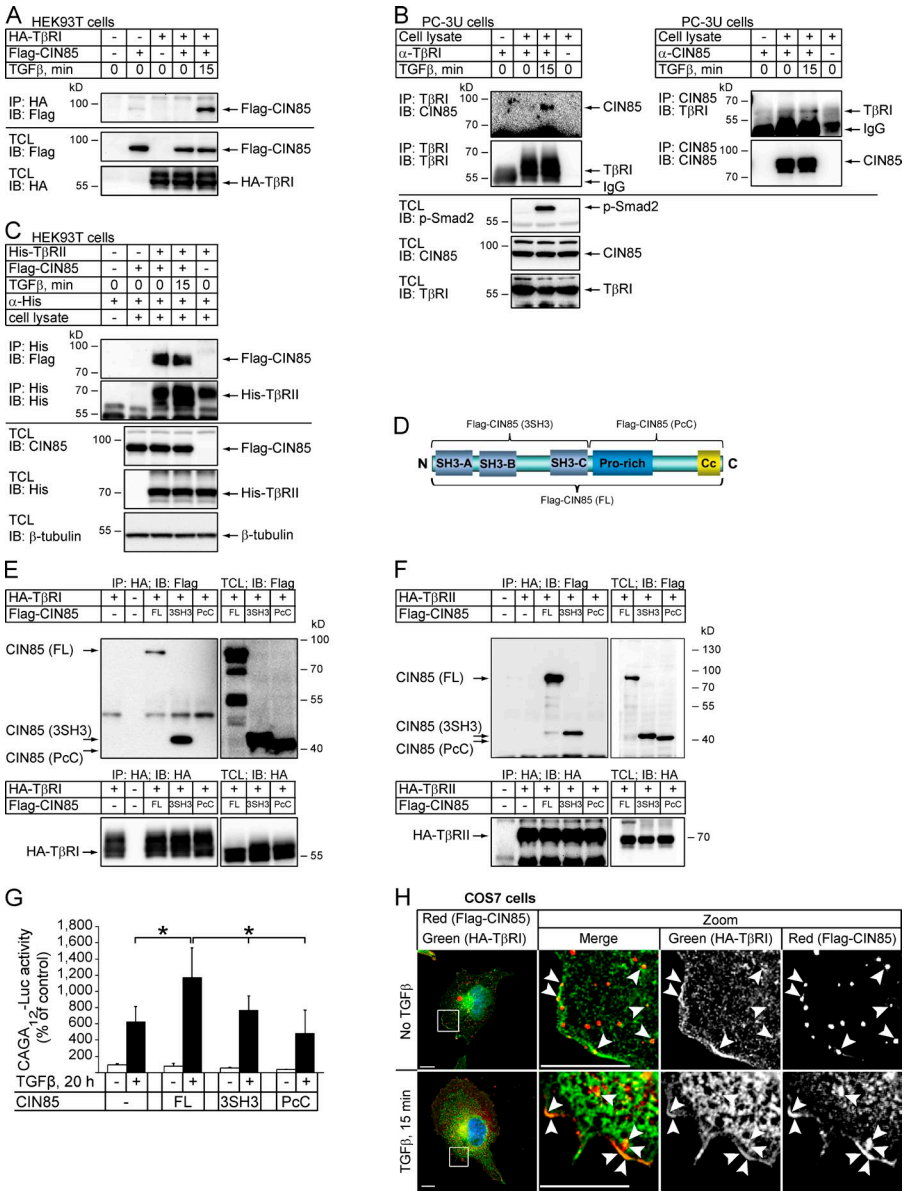

Figure 4. **CIN85 interacts with TGFβ receptors.** (A) HEK293T cells were transfected with Flag-CIN85 in the absence or presence of HA-TβRI and incubated with 5 ng/ml TGFβ for 15 min, as indicated. The cell lysates were subjected to immunoprecipitation with HA antibodies followed by blotting with Flag antibodies. The levels of HA-TβRI and Flag-CIN85 expression were determined by immunoblotting of total cell lysates. (B) PC-3U cells were treated with 5 ng/ml TGFβ for 15 min and endogenous TβRI (left) or CIN85 (right) were immunoprecipitated with 1 µg of goat anti-TβRI or rabbit anti-CIN85 antibodies, respectively. Immunoprecipitates were analyzed by immunoblotting for the presence of CIN85 or TβRI, as indicated. Total cell lysate was also subjected to immunoblotting for CIN85 and TβRI, and for phosphorylated Smad2 to determine activation of TGFβ signaling (bottom). (C) HEK293T cells were transfected with Flag-CIN85 in the absence or presence of His-TβRII and incubated with 5 ng/ml TGFβ for 15 min, as indicated. TβRII was immunoprecipitated from the cell lysates with His antibodies. Coimmunoprecipitated CIN85 and immunoprecipitated TβRII were detected by immunoblotting with Flag and His antibodies, respectively. The levels of His-TβRII and Flag-CIN85 expression were determined by immunoblotting of total cell lysates. (D) Schematic illustration of the CIN85 molecule. The full-length molecule (FL) and the parts of CIN85 included into the deletion mutants containing three SH3 domains (3SH3) or proline-rich and coiled-coil domains (PcC) are indicated. (E) TβRI interacts with the N-terminal part of CIN85. HA-TβRI was transfected into HEK293T cells together with full-length Flag-CIN85 or with deletion mutants including three SH3 domains (3SH3) or proline-rich and coiled coil domains (PcC). The cells were incubated with 5 ng/ml TGFβ for 15 min and TβRI was immunoprecipitated from the cell lysates with HA antibodies. The coimmunoprecipitated CIN85 or CIN85 deletion mutants were detected by immunoblotting with Flag antibodies. The expression of HA-TβRI and Flag-CIN85 molecules was determined by immunoblotting of total cell lysates. (F) TβRII interacts with the N-terminal part of CIN85. HA-TβRII was transfected into HEK293T cells together with full-length Flag-CIN85 or with its deletion mutants. The cells were treated as in E and TβRII was immunoprecipitated from the cell lysates with HA antibodies. The coimmunoprecipitated CIN85 or CIN85 deletion mutants were detected by immunoblotting with Flag antibodies. (G) The transcriptional activity of TGFβ is enhanced by full-length CIN85 but not by its N- or C-terminal fragments. HEK293T cells, transfected with $CAGA_{12}$-Luc and full-length CIN85 or its N- or C-terminal parts, were treated (shaded bars) or not (open bars) with TGFβ (5 ng/ml) for 20 h. Luciferase activity was measured and transfection efficiency was normalized to β-galactosidase activity. The results are presented as the mean (in percentage of control) of three independent experiments. Error bars are SD. *, $P < 0.05$. (H) COS7 cells were grown on cover glasses and transfected with HA-TβRI and Flag-CIN85. 24 h after transfection, the cells were transferred to serum-low culture medium and starved for 16 h. Then cells were treated with TGFβ (5 ng/ml; 15 min), fixed, permeabilized, and incubated with rabbit HA antibodies and mouse Flag antibodies. HA-tagged receptor (green) and Flag-CIN85 (red) were detected by binding Alexa Fluor 488–conjugated anti-rabbit IgG and Alexa Fluor 555–conjugated anti–mouse IgG secondary antibodies, respectively. Sites of colocalization are indicated by arrowheads. Bars, 10 µm.

Havrylov et al., 2010). We therefore studied if the effect of CIN85 on TGFβ signaling could be explained by modulation of TβRI location. We separated the postnuclear supernatants of PC-3U cells transfected with HA-TβRI alone or together with Flag-CIN85 by centrifugation in discontinuous iodixanol gradient (Fig. 6 A). Immunoblot analysis of the fractions showed that most of HA-TβRI (~80%) was localized at the 30–20% or the 20–10% iodixanol interfaces enriched for EEA1- and Rab7-positive vesicles, respectively (Fig. 6, A and B). Overexpression of CIN85 resulted in the appearance of detectable amounts of HA-TβRI in light fractions at the 10–0% iodixanol interface enriched for Rab11-positive vesicles (Fig. 6, A and B). Analysis of these fractions for the presence of biotinylated cell surface proteins revealed that they contained plasma membrane as well (Fig. 6 C), which is in accordance with a previous study (Zhu et al., 2012). We also obtained a similar effect of CIN85 overexpression on the distribution of HA-TβRI in an iodixanol gradient using postnuclear supernatants from HEK293T cells (Fig. S3, A and B). Treatment of these cells with TGFβ for 15 min did not change the distribution of the receptor (Fig. 3, A

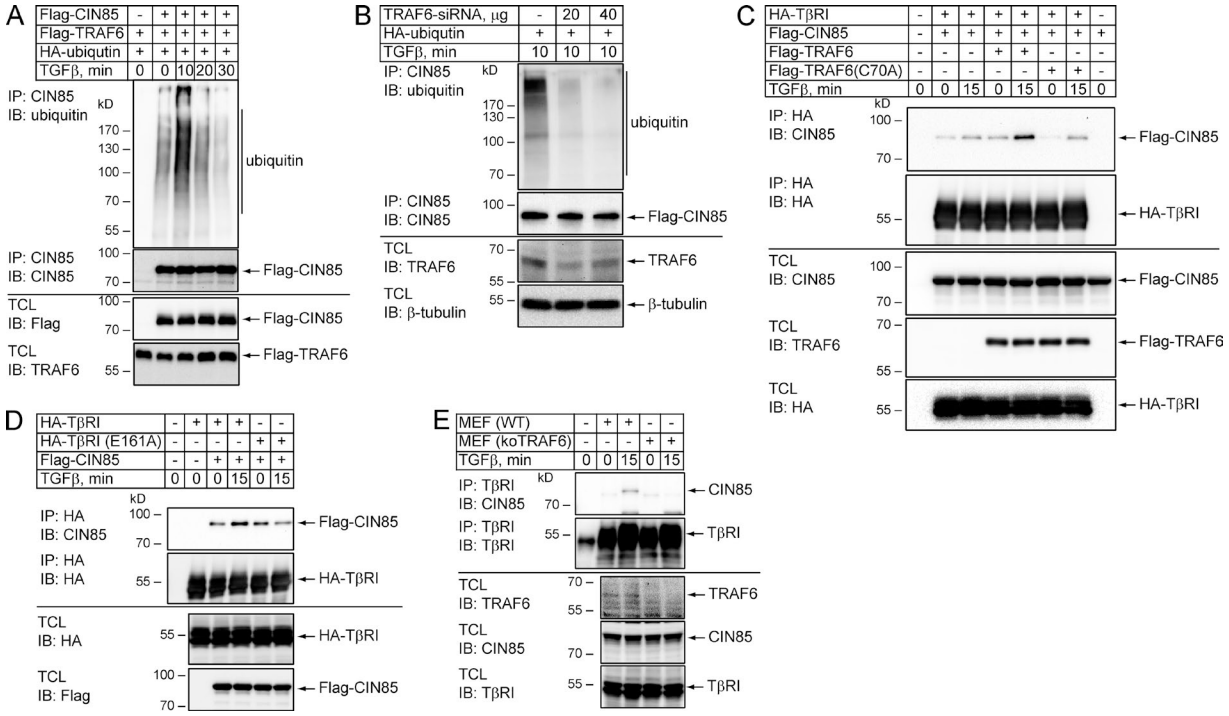

Figure 5. **TRAF6 ubiquitinates CIN85 and enhances the interaction between TβRI and CIN85.** (A) HEK293T cells were cotransfected with Flag-CIN85, Flag-TRAF6, and HA-ubiquitin and treated with 5 ng/ml TGFβ for the indicated time periods. The cell lysates were subjected to immunoprecipitation with CIN85 antibodies followed by immunoblotting with polyubiquitin antibodies. The expression of the proteins under investigation was determined by immunoblotting total cell lysates. (B) HEK293T cells were transfected with control siRNA or TRAF6-siRNA, as well as with HA-ubiquitin, and treated with 5 ng/ml TGFβ for 10 min. The cell lysates were subjected to immunoprecipitation using CIN85 antibodies followed by immunoblotting with polyubiquitin antibodies. The efficiency of TRAF6 knockdown and equality of protein loading were analyzed by immunoblotting of total cell lysates. (C) HEK293T cells were cotransfected with HA-TβRI and Flag-CIN85, in the absence or presence of Flag-TRAF6 or E3-ligase-deficient Flag-TRAF6(C70A) mutant, and treated with 5 ng/ml TGFβ for 15 min, as indicated. Cell lysates were subjected to immunoprecipitation with HA antibodies followed by immunoblotting with Flag or HA antibodies. The expression of the proteins under investigation was determined by immunoblotting of total cell lysates. (D) HEK293T cells were cotransfected with Flag-CIN85 and HA-TβRI or HA-TβRI(E161A) mutant and treated with 5 ng/ml TGFβ for 15 min, as indicated. Cell lysates were subjected to immunoprecipitation with HA antibodies followed by immunoblotting with Flag or HA antibodies. The expression of proteins was evaluated by immunoblotting of total cell lysates. (E) Wild-type or TRAF6-deficient mouse embryonic fibroblasts (MEFs) were treated with 5 ng/ml TGFβ for 15 min. Cell lysates were subjected to immunoprecipitation with anti-TβRI antibodies, followed by immunoblotting for CIN85. Total cell lysates were also subjected to immunoblotting for endogenous TRAF6, CIN85, and TβRI.

and B). In addition, immunofluorescence staining showed that in PC-3U cells deprived of CIN85 by siRNA transfection, endogenous TβRI was concentrated in intracellular compartments, whereas in cells with normal level of CIN85, the distribution of the receptor was more even throughout the cell (Fig. 6 D). These results suggested that CIN85 may be involved in the regulation of the subcellular localization of TβRI.

By biotinylating cell surface proteins, we found that more TβRI and TβRII were pulled down with neutravidin agarose beads from lysates of HEK293T cells (Fig. 7 A) or PC-3U cells (Fig. 7 B), which overexpressed CIN85, compared with control cells. These data were consistent with the results we obtained using iodixanol density gradient membrane flotation assays and suggested that CIN85 promotes the presentation of TGFβ receptors on the cell surface. Notably, the biotinylation assay showed that the amount of HA-TβRI on the surface of both control and CIN85-transfected cells was not affected by treatment with TGFβ, at least for the first two hours (Fig. 7 C).

Increased amount of available TGFβ receptors on the surface of CIN85-overexpressing cells could explain the stronger response to ligand stimulation. We expressed the C- or N-terminal fragments of CIN85 in HEK293T cells and determined their effects on the amount of HA-TβRI on the cell surface, compared with the effect of full-length CIN85. None of the CIN85 fragments could increase cell surface expression of TβRI (Fig. 7 D). These results are consistent with the observation that only full-length CIN85 strengthens cellular responses to TGFβ (Fig. 4 E). They also support the notion that the enhancing effect of CIN85 on TGFβ signaling is caused by the higher amount of the receptors on the cell surface.

The effect of CIN85 on TGFβ signaling is blocked by dominant-negative Rab11

We did not observe any effect of CIN85 overexpression on the total amount of TGFβ receptors (see, e.g., Fig. 7 A, bottom), whereas the results of fractionation in density gradient (Fig. 6) supported the possibility that CIN85 alters their intracellular localization. It has been proposed that clathrin-mediated endocytosis of TGFβ receptors promotes TGFβ signaling, whereas internalization through lipid rafts/caveolae negatively modulates TGFβ signaling by promoting TGFβ receptor degradation (Di Guglielmo et al., 2003; Chen, 2009). As CIN85 has been shown to interact with components of clathrin-coated pits, we examined whether its enhancing effect on TGFβ signaling can be explained by a shift to clathrin-mediated internalization of TβRI. However, we could not detect any significant effect of CIN85 overexpression on the distribution of TβRI between caveolin-1–positive fractions and nonraft membrane fractions (Fig. S3 C).

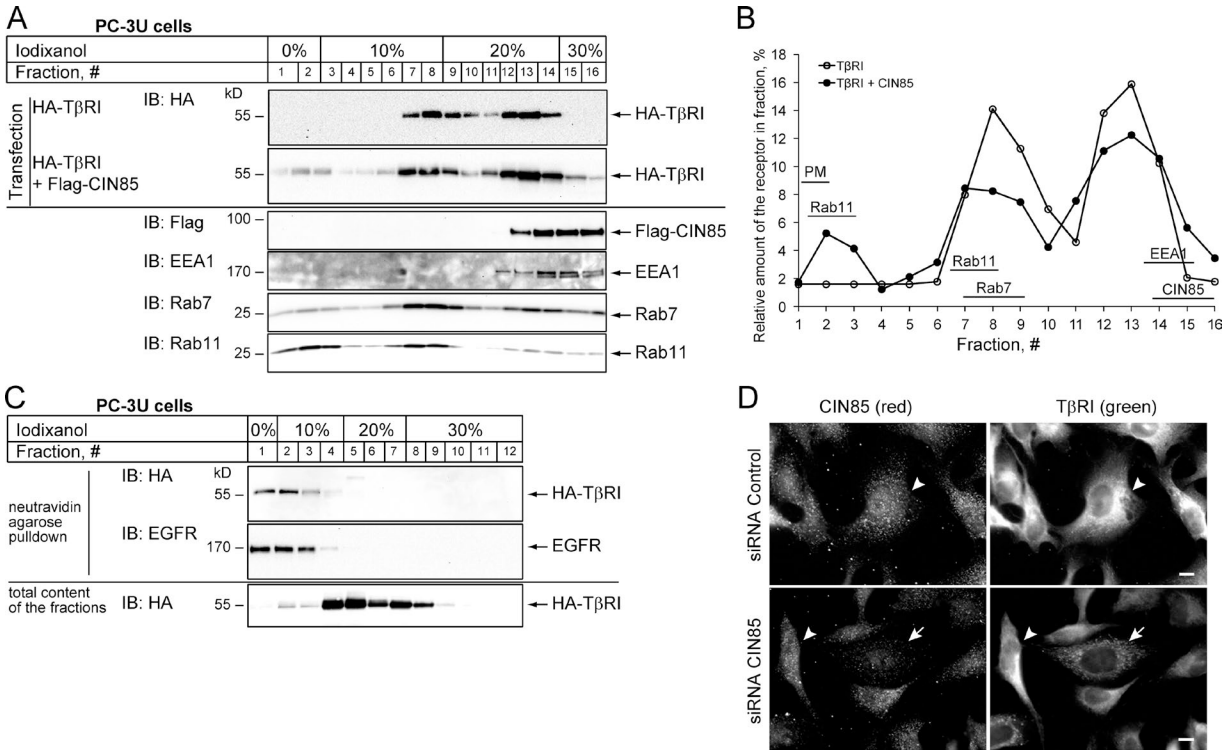

Figure 6. **CIN85 alters the compartmentalization of TβRI.** (A) PC-3U cells were transfected with HA-TβRI alone or in combination with Flag-CIN85. 48 h after transfection, cells were homogenized and subcellular membrane vesicles were separated by iodixanol density gradient ultracentrifugation, as described in Materials and methods. Equal volumes of each fraction were separated by SDS-PAGE and analyzed by immunoblotting with antibodies against HA to detect HA-TβRI. Marker proteins for different membrane vesicles, including EEA1 for early endosomes, Rab7 for late endosomes, and Rab11 for recycling endosomes, were used to locate the migration of these membrane vesicles along the density gradients. CIN85 was analyzed in the fractions by blotting with Flag antibodies. (B) Quantification of the immunoblots of HA-TβRI presented in A showing that coexpression of CIN85 resulted in an increased amount of the receptor in the upper fractions of iodixanol gradient. The intensity of HA-positive signal in each fraction was quantified using the Quantity One software. The sum of HA-positive signals from all fractions was set as 100%. The location of each marker protein is indicated. PM, plasma membrane. The data shown are from a representative experiment out of four repeats. (C) Cell surface proteins migrate at the top of the density gradient. Proteins on the cell surface of PC-3U cells transfected with HA-TβRI were labeled with biotin and then the subcellular membrane vesicles were separated by iodixanol density gradient ultracentrifugation. Biotinylated proteins from each fraction were precipitated with neutravidin-agarose beads and analyzed by immunoblotting with HA and EGFR antibodies. The total amount of HA-TβRI was determined by subjecting the whole fraction to immunoblotting using HA antibodies. (D) Endogenous TβRI is sequestered in intracellular compartments in cells with down-regulated CIN85 expression. PC-3U cells were grown on cover glasses and transfected with control siRNA or CIN85-siRNA. 72 h after transfection the cells were fixed, permeabilized, and incubated with goat anti-TβRI and rabbit anti-CIN85 antibodies. TβRI (green channel) and CIN85 (red channel) were visualized by binding Alexa Fluor 488–conjugated anti–goat and Alexa Fluor 555–conjugated anti–rabbit antibodies, respectively. Cells with a lower amount of CIN85 are indicated by arrows. Arrowheads indicate cells containing a normal level of CIN85. Bars, 10 µm.

TGFβ receptors internalized via clathrin-coated pits are recycled back to the plasma membrane through a Rab11-dependent mechanism (Mitchell et al., 2004). The possibility that TβRI recycling was affected by CIN85 was investigated by a biotinylation assay (Fig. S4). TβRI at the cell surface was first biotinylated by sulfo-NHS-SS-biotin. Cells were then incubated for 30 min at 37°C, and thereafter biotin was stripped from extracellular proteins by incubation in a reducing agent. 87% of the biotinylated receptor remained internalized in control cells (Fig. S4, lane 3), whereas cells that overexpressed CIN85 contained only 66% of the biotinylated receptor intracellularly (Fig. S4, lane 8), suggesting that CIN85 promoted recycling of the receptor back to the cell surface. We therefore investigated whether enhancement of TGFβ signaling by CIN85 was affected by interfering with Rab11 activity. Overexpression of a dominant-negative myc-Rab11(S25N) mutant in HEK293T cells decreased the amount of biotinylated HA-TβRI on the cell surface under steady-state conditions (Fig. 8 A), consistent with previously reported data (Mitchell et al., 2004). In cells transfected with myc-Rab11(S25N), overexpression of CIN85 did not increase the level of TβRI on the cell surface (Fig. 8 A). Moreover, the enhancement of TGFβ-induced $CAGA_{12}$-Luc reporter activation by CIN85 overexpression was abolished by expression of the dominant-negative Rab11 mutant (Fig. 8 B). Rab11 was coimmunoprecipitated with wild-type CIN85, but not with the truncated mutants of CIN85 (Fig. 8 C). A dominant-negative mutant of Rab4, which does not regulate TGFβ receptor recycling (Mitchell et al., 2004), did not prevent CIN85-regulated increasing of TβRI on the cell surface (Fig. 8 D). Together, these data suggest that CIN85 is involved in the Rab11-dependent trafficking of TβRI to the plasma membrane.

Expression of CIN85 is increased in prostate tumors

It is known that prostate tumors express high levels of TGFβ (Thompson et al., 1992) and that TGFβ signaling is activated in many tumors, especially in the late stages of tumorigenesis (Massagué, 2008; Heldin and Moustakas, 2012; Mu et al., 2012). We investigated whether expression of CIN85 correlates with the development of prostate cancer. Histological analysis

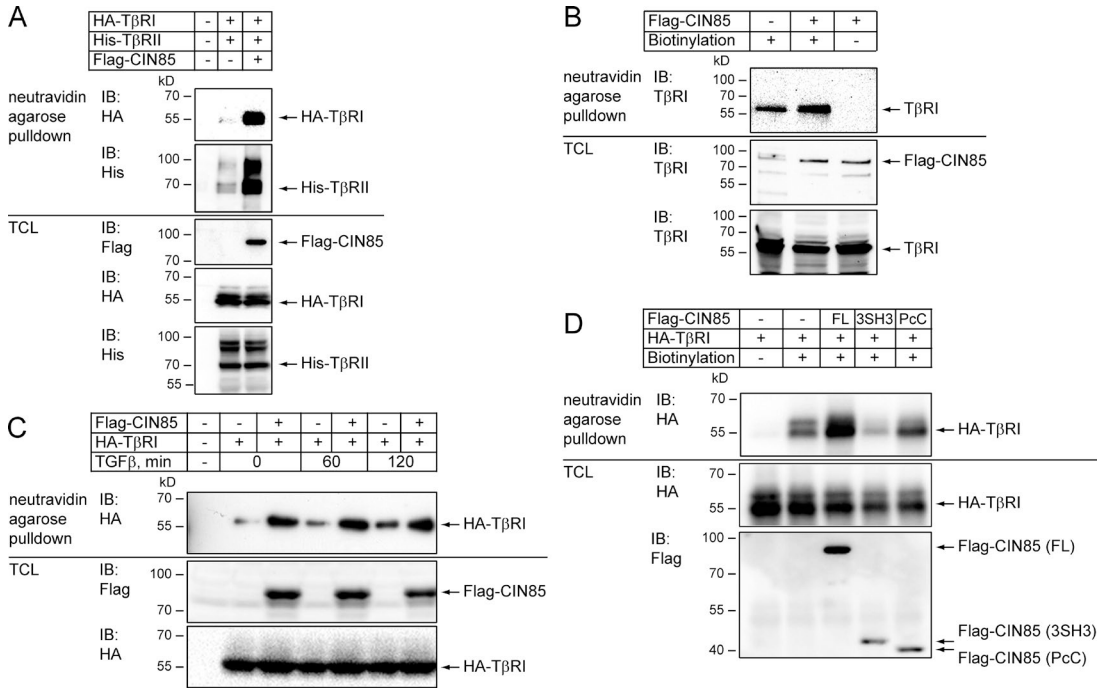

Figure 7. **CIN85 increases the amount of TβRI and TβRII on the cell surface.** (A) Overexpression of CIN85 in HEK293T cells increases the amount of TβRI and TβRII at the cell surface. HEK293T cells were transfected with HA-TβRI and His-TβRII in the absence or presence of Flag-tagged CIN85, as indicated. 48 h after transfection, cell surface proteins were biotinylated and isolated by incubation with neutravidin-agarose beads, as described in Materials and methods, and the amount of HA-TβRI and His-TβRII was analyzed by immunoblotting with HA and His antibodies, respectively. The levels of HA-TβRI, His-TβRII, and Flag-CIN85 expression were determined by immunoblotting total cell lysates. (B) Overexpression of CIN85 in PC-3U cells increases the amount of endogenous TβRI on the cell surface. PC-3U cells that either overexpressed CIN85 or did not were prepared, as described in Fig. 3 A. The cell surface proteins were biotinylated and precipitated by neutravidin-agarose beads. The precipitates were analyzed for the presence of endogenous TβRI by immunoblotting with rabbit anti-TβRI antibodies. Expression of CIN85 and TβRI was evaluated by immunoblotting of total cell lysates with the indicated antibodies. CIN85-overexpressing cells not labeled with biotin were used as a control for pull-down specificity. (C) The effect of CIN85 on cell surface expression of HA-TβRI does not depend on ligand treatment. HEK293T cells were transfected with HA-TβRI in the absence or presence of Flag-tagged CIN85 and incubated with 5 ng/ml TGFβ for 0, 60, and 120 min. Cell surface proteins were biotinylated and isolated by neutravidin-agarose pull-down, and the amount of the HA-TβRI was analyzed by immunoblotting with HA antibodies. The levels of HA-TβRI and Flag-CIN85 expression were determined by immunoblotting of total cell lysates. (D) Full-length CIN85 is necessary to promote TβRI expression at the cell surface. HEK293T cells were transfected with HA-TβRI and full-length CIN85 or its truncated mutants, as indicated. 48 h after transfection biotinylated cell surface proteins were isolated by neutravidin-agarose pull-down, and the amount of HA-TβRI brought down was analyzed by immunoblotting. HA-TβRI–overexpressing cells that had not been treated with biotin were used as a control for pull-down specificity. The expression of transfected proteins was evaluated by immunoblotting of total cell lysates.

of prostate tumor tissues from patients showed that expression of CIN85 positively correlated with the severity of the disease (Fig. 9, A and B). We also observed much higher levels of phospho-Smad2 in aggressive prostate cancer tissues when compared with normal prostate, and a high level of phosphorylated Smad2 corresponded with high levels of CIN85 in the same tissue (Fig. S5). These results suggest a correlation between the level of CIN85 expression and activation of TGFβ signaling in prostate cancers.

Interestingly, we found that treatment of PC-3U cells with TGFβ resulted in higher levels of CIN85 mRNA (Fig. 10 A) and protein (Fig. 10 B). These observations suggest the existence of a positive feedback mechanism by which activation of TGFβ receptors results in elevation of CIN85 expression, which in turn enhances TGFβ signaling.

Discussion

We have shown in this paper that CIN85 forms a complex with TGFβ receptors and that the E3 ubiquitin ligase TRAF6 promotes its interaction with TβRI in a TGFβ-dependent manner (Fig. 4, A–C; and Fig. 5, C and D). Overexpression of CIN85 resulted in a greater amount of TGFβ receptors on the cell surface (Fig. 7, A and B), but did not cause any significant changes in the total amount of TGFβ receptors. Dominant-negative Rab11 abolished the effect of CIN85 (Fig. 8, A and B), which, together with the results of a TβRI cell surface biotinylation assay (Fig. S4), supports the notion that CIN85 regulates TβRI recycling. The inability of dominant-negative Rab4 mutant to prevent the effect of CIN85 suggests that CIN85 does not direct TβRI to the fast recycling route that is regulated by Rab4, but rather enhances its recycling through the Rab11-controlled route. We cannot exclude the possibility that the increased number of TGFβ receptors on the cell surface is also a result of enhanced trafficking of newly synthesized receptors to the plasma membrane, which has been proposed to be modulated by CIN85 for other proteins (Havrylov et al., 2010). The increased number of TGFβ receptors at the cell surface may explain why CIN85 expression makes cells more sensitive to TGFβ treatment (Figs. 1, 2, and 3), as TGFβ responsiveness has been shown to correlate with the cell surface receptor levels (Xu et al., 2012).

Knockdown of CIN85 by siRNA resulted in trapping of TβRI in intracellular compartments, but not on the cell surface (Fig. 6 D). This observation further supports the notion that

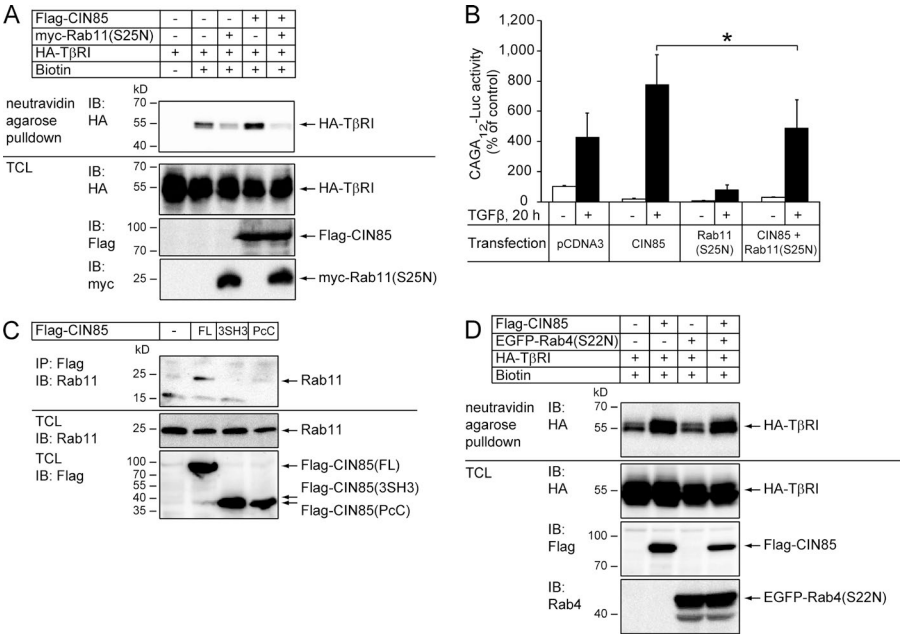

Figure 8. **Dominant-negative Rab11 inhibits the effect of CIN85 on TGFβ signaling.** (A) HEK293T cells were transfected with HA-TβRI, Flag-CIN85, and the dominant-negative myc-Rab11(S25N) mutant, as indicated. 48 h after transfection, cell surface proteins were biotinylated and isolated by neutravidin-agarose pull-down. The amount of biotinylated HA-TβRI was analyzed by immunoblotting with HA antibodies. Cells transfected with HA-TβRI, but not treated with biotin, were used as a control for specificity of neutravidin-agarose pull-down. The levels of HA-TβRI, Flag-CIN85, and myc-Rab11(S25N) expression were determined by immunoblotting of total cell lysates. (B) HEK293T cells that had been transfected with $CAGA_{12}$-Luc, Flag-CIN85, and myc-Rab11(S25N), as indicated, were either treated with TGFβ (5 ng/ml) for 20 h (shaded bars) or not (open bars), and the luciferase activity in the cell lysates was measured. Transfection efficiency was normalized to β-galactosidase activity. The data are presented as the mean (in percentage of control) of six independent experiments. Error bars are SD. *, $P < 0.05$. (C) HEK293T cells were transfected with full-length Flag-CIN85 or with its deletion mutants that encompassed the three SH3 domains (3SH3) or the proline-rich and coiled-coil domains (PcC). The cell lysates were subjected to immunoprecipitation with Flag antibodies, followed by blotting with Rab11 antibodies. The expression levels were determined by immunoblotting of total cell lysates with Rab11 and Flag antibodies. (D) Dominant-negative Rab4 does not inhibit the effect of CIN85 on the cell surface expression of TβRI. HEK293T cells were transfected with HA-TβRI, Flag-CIN85, and the dominant-negative Rab4 mutant, as indicated. 48 h after transfection, cell surface proteins were biotinylated and isolated by neutravidin-agarose pull-down. The amount of biotinylated HA-TβRI on the cell surface was analyzed by immunoblotting with HA antibodies. The levels of HA-TβRI, Flag-CIN85, and Rab4 expression were determined by immunoblotting of total cell lysates.

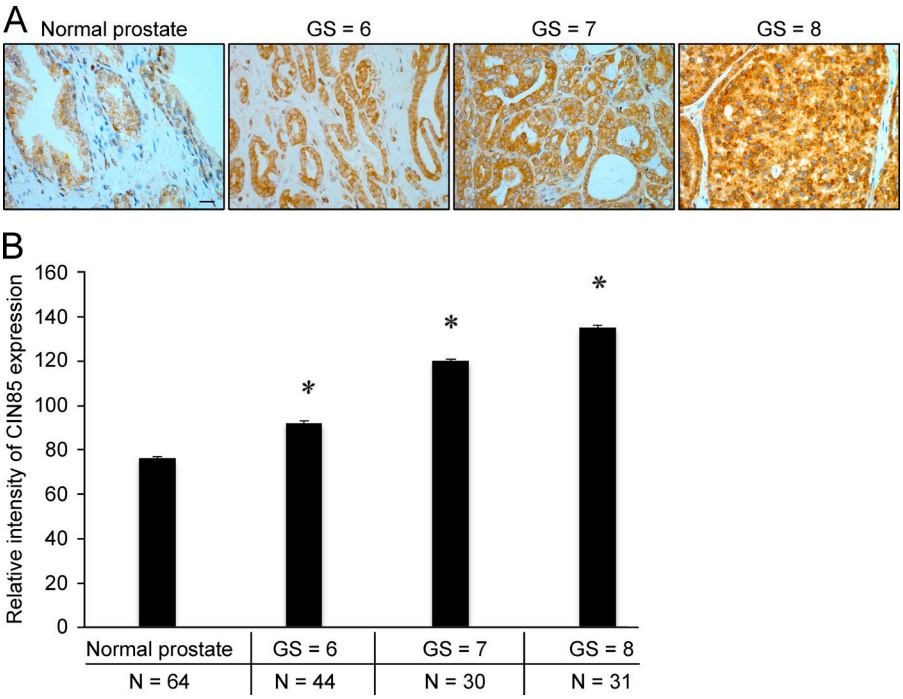

Figure 9. **CIN85 expression correlates with malignancy of prostate cancers.** (A) Normal prostate and tumor tissues at different malignancy grades were stained with anti-CIN85 antibodies. Bar, 20 μm. GS, Gleason score. (B) Quantification of CIN85 expression in different prostate tissues shows a positive correlation between tumor grade and amount of CIN85. Error bars represent SEM. *, $P < 0.05$, compared with normal tissue.

CIN85 is primarily involved in the regulation of TβRI recycling, but not in its internalization. In a similar manner, the recycling of TβRII was blocked by down-regulation of Dab2, another adaptor protein (Penheiter et al., 2010). It has been shown that Dab2 makes complexes with CIN85 on the plasma membrane and that they dissociate from each other upon EGF stimulation (Kowanetz et al., 2003). We explored the possibility that Dab2 and CIN85 work together to control TβRI recycling. However, overexpression of mutant Dab2R699A, which cannot bind CIN85 (Kowanetz et al., 2003), had no effect on the enhancement of TGFβ signaling by CIN85 (unpublished data). Thus, it seems that these proteins regulate different events in the trafficking of TGFβ receptors, which agrees with the finding that the transport of TβRI and TβRII

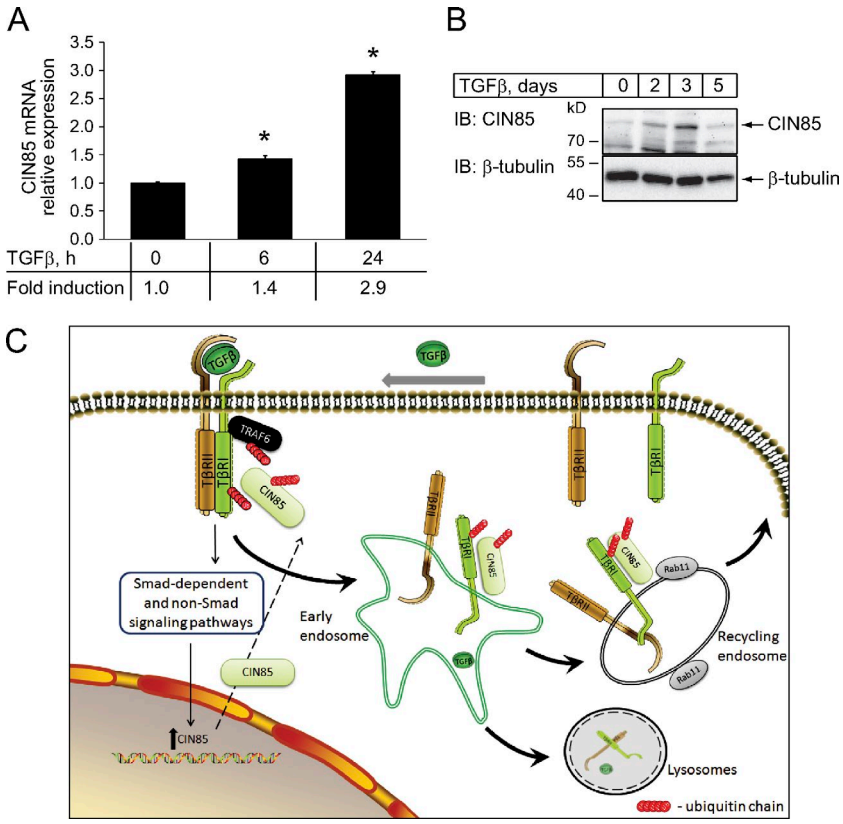

Figure 10. **TGFβ induces CIN85 mRNA and protein expression.** (A) PC-3U cells were stimulated with TGFβ for 0, 6, and 24 h. The DNA was extracted and the expression of CIN85 mRNA (SH3KBP1; GenBank accession no. NM_031892.2) was analyzed by qRT-PCR. The values were normalized to GAPDH mRNA and plotted as the mean fold induction of TGFβ-stimulated mRNA levels relative to unstimulated levels (0 h was set to 1). Error bars correspond to SD values determined from triplicate measurements. *, $P < 0.05$ cells treated with TGFβ compared with untreated cells. (B) PC-3U cells were incubated in the presence of 5 ng/ml TGFβ for the indicated time periods. Cell lysates were analyzed for the expression of CIN85 by immunoblotting with anti-CIN85 antibodies. The membrane was stripped and probed with β-tubulin antibodies for loading control. (C) Schematic illustration of the proposed role of CIN85 in TGFβ signaling. Upon ligand-induced activation of TGFβ receptors, TRAF6 becomes autoubiquitinated and ubiquitinates TβRI and CIN85. CIN85 binds to TβRI and this complex is stabilized by the ubiquitin chains on TβRI, CIN85, and/or TRAF6. Formation of such a complex enhances the recycling of receptors through a Rab11-dependent route and increases their amount on the plasma membrane. This results in higher responsiveness of the cells to TGFβ. The activation of the TGFβ signaling pathway also increases expression of CIN85, providing a positive feedback loop.

back to the cell surface is dependent on two distinct recycling pathways (Gleason et al., 2014). It has been shown that CIN85 affects the recycling of EGFR through interaction with the Arf GTPase-activating protein ASAP1 (Kowanetz et al., 2004). It remains to be determined if ASAP1 is also involved in CIN85-modulated trafficking of TβRI.

The E3 ubiquitin ligase TRAF6 strongly enhanced the TGFβ-induced interaction between CIN85 and TβRI, as demonstrated by coimmunoprecipitation experiments (Fig. 5, C and D). CIN85 has previously been shown to interact with TRAF1 and TRAF2, but not with TRAF6 (Narita et al., 2005). We found that the interaction between TβRI and CIN85 was enhanced only by wild-type TRAF6, but not by a TRAF6 ubiquitin ligase–deficient mutant (Fig. 5 C). TGFβ-induced oligomerization of TGFβ receptors leads to autoubiquitination of TRAF6, which in turn activates the MAPK kinase kinase TAK1 and the MKK3/6–p38 pathway (Sorrentino et al., 2008). We have shown that TβRI is also ubiquitinated by TRAF6 (Mu et al., 2011; Sundar et al., 2015); given that all three SH3 domains of CIN85 bind to ubiquitin (Bezsonova et al., 2008), it is possible that polyubiquitin chains mediate the binding of CIN85 to the receptor complex. The role of TβRI ubiquitination in the regulation of its intracellular trafficking remains to be explored further, as it can also promote the cleavage of the receptor's intracellular domain and its translocation to the nucleus (Mu et al., 2011).

The interaction between TβRI and CIN85 was found to be promoted by TGFβ stimulation (Figs. 4 and 5). However, the finding that overexpression of CIN85 by itself made cells more sensitive to TGFβ stimulation (Fig. 1) suggests that there may be a low affinity interaction between TβRI and CIN85 before TGFβ stimulation. The TGFβ-induced stabilization of the interaction would then serve as an amplification mechanism.

We found that TGFβ induces expression of CIN85 in cultured cells (Fig. 10, A and B). This suggests the existence of a positive feedback loop, where TGFβ induces the expression of CIN85, which in turn enhances the responsiveness of cells to TGFβ. Interestingly, expression of CIN85 correlates with the malignancy of prostate cancers (Fig. 9, A and B) and with increased TGFβ activity, as visualized by the staining of phosphorylated Smad2 in aggressive prostate cancer tissues (Fig. S5). This further supports the notion that CIN85 is part of an amplification mechanism that contributes to progression of prostate cancers by increasing TGFβ signaling.

In summary, we have demonstrated that CIN85 enhances TGFβ-induced signaling and cellular responses to TGFβ (Fig. 10 C). CIN85 interacts with TGFβ receptors in a TRAF6-dependent manner and increases the exposure of TβRI on the cell surface by promoting receptor recycling. The positive effect of CIN85 on TGFβ signaling together with the observed expression of CIN85 in malignant prostate cancer cells are of potential importance for the understanding of the mechanisms that control cancer progression.

Materials and methods

Cell culture and transfection

HEK293T and COS7 cells (ATCC) were cultured in DMEM supplemented with 10% FBS, glutamine, and antibiotics. The PC-3U human prostatic carcinoma cell line was obtained from S. Nilsson (University Hospital, Uppsala, Sweden) and represents a clone from the original PC-3 cell line (ATCC; Franzén et al., 1993). The cells were cultured in RPMI medium supplemented with 10% FBS, 1% glutamine, and 1% penicillin-streptomycin. All cell cultures were incubated at 37°C in the presence of 5% CO_2. For TGFβ stimulation experiments, PC-3U cells

were starved for 16 h in 0.1% FBS in RPMI. HEK293T and COS7 cells were starved for 16 h in 1% FBS in DMEM. Cells were then stimulated with 5 ng/ml TGFβ.

Plasmids and siRNAs

Expression vectors encoding Flag-CIN85, Flag-CIN85(3SH3), and Flag-CIN85(PcC) in pcDNA3 vector, and GST-CIN85(SH3ABC), GST-CIN85(SH3A), GST-CIN85(SH3B), and GST-CIN85(PcC) in pGEX-4T-1 vector, were provided by I. Dikic (Goethe University, Frankfurt am Main, Germany; Soubeyran et al., 2002). In brief, the FLAG-CIN85 construct encodes amino acids 1–665 of CIN85 (UniProt accession no. Q96B97), the Flag-CIN85(3SH3) construct encodes amino acids 1–332, and the Flag-CIN85(PcC) construct encodes amino acids 327–665 of CIN85. GST-CIN85(SH3A) and GST-CIN85(SH3B) encode individual SH3 domains of CIN85 (amino acids 1–83 and 79–217, respectively), the GST-CIN85(SH3ABC) construct encodes all three SH3 domains of CIN85 (amino acids 1–332), and GST-CIN85(PcC) contains only the proline-rich region and the coiled-coil motif of CIN85 (amino acids 327–665).

The plasmid pCDNA3-TβRI-HA for expression of full-length TβRI (UniProt accession no. P36897) with an HA tag fused to the C terminus was provided by P. ten Dijke (University of Leiden, Leiden, Netherlands) and plasmid pCMV5-TβRII-His for expression of full-length TβRII (UniProt accession no. P37173) with 6XHis tag at the C terminus was obtained from J. Massagué (Memorial Sloan-Kettering Cancer Center, New York, NY). Constructs of N-terminal Flag-tagged mouse wild-type TRAF6 (UniProt accession no. P70196) and its E3 ligase–deficient mutant (Flag-TRAF6 C70A) cloned into pCDNA3-1 vector were gifs from Zhijian J. Chen (University of Texas Southwestern Medical Center, Dallas, TX). Plasmid pCDNA3.1-3XHA ubiquitin for expression of N-terminal HA-tagged ubiquitin was a gift from V.M. Dixit (Genentech, San Francisco, CA). The plasmid PCMV-intron-myc-Rab11S25N for expression of a dominant-negative mutant of Rab11A (UniProt accession no. P62491 was purchased from Addgene. The plasmid pEGFP-Rab4AS22N for expression of GTPase-defective Rab4A (UniProt accession no. P20338) was a gift from C. Hellberg (University of Birmingham, Birmingham, UK; Karlsson et al., 2006).

The CAGA12 luciferase reporter vector was generated using the pGL3 basic plasmid (Promega) by inserting 12 tandem copies of the CAGA Smad binding element upstream of the adenovirus major late promoter driving luciferase gene expression (Dennler et al., 1998). The ARE luciferase reporter vector was generated using pGL5ti plasmid by inserting two tandem copies of the activin-responsive element (Chen et al., 1996). Plasmid pCMV-LacZ for expression of β-galactosidase was purchased from Takara Bio Inc.

To knock down CIN85 expression, we used Silencer Select siRNA (5′-GACUGUUACCAUAUCCCAAtt-3′; Life Technologies), and nontargeting Silencer Select Negative Control No.1 siRNA (Life Technologies) was used as negative control. SMARTpool siGENOME Human TRAF6 (7189) siRNA (M-004712-00-0020) for the knockdown of TRAF6 and siGENOME Non-Targeting siRNA #4 (D-001210-04-05) used as a control were obtained from GE Healthcare.

For transient transfections, cells were seeded at 60% density in the corresponding culture medium. Cells were transfected with plasmid DNAs using FuGENE HD (Roche) and with siRNAs using siLentFect reagent (Bio-Rad Laboratories) according to the manufacturers' protocols. Transfection media were replaced with fresh media after 24 h.

Antibodies and reagents

Antibodies against the following proteins were used for immunoblotting (IB) or immunofluorescence (IF): rabbit anti-CIN85 antibody (diluted 1:500 for IB and 1:200 for IF) was obtained from Proteintech; mouse anti-His antibody (diluted 1:2,000) was obtained from Takara Bio Inc.; rabbit anti-HA (Y-11; diluted 1:500 for IB and 1:50 for IF), mouse anti-ubiquitin (P4D1; diluted 1:400), and rabbit anti-TβRI (V22; diluted 1:500 for IB and 1:50 for IF) antibodies were obtained from Santa Cruz Biotechnology, Inc.; rabbit anti–phospho-p38 MAPK (D3F9, 4511; diluted 1:1,000) and mouse anti-p38 MAPK (5F11, 9217; diluted 1:1,000) antibodies were obtained from Cell Signaling Technology. Mouse anti-Rab11 antibody (diluted 1:1,000 for IB and 1:500 for IF) was obtained from BD and rabbit anti-Smad2 antibody (diluted 1:1,000) was obtained from Epitomics. Rabbit antibody against TRAF6 (diluted 1:500) was obtained from Life Technologies. Mouse antibody against β-tubulin (diluted 1:1,000), mouse anti-HA (HA7; 1:1,000), and mouse anti-Flag (M2; diluted 1:1,000) antibodies were obtained from Sigma-Aldrich. Rabbit anti–phospho-Smad2 antiserum (diluted 1:500) was generated in house by immunizing rabbits with a peptide KKK-SSpMSp coupled to keyhole limpet hemocyanin, as described previously (Persson et al., 1998). Alexa Fluor–labeled anti-goat antibodies for IF were purchased from Invitrogen and used at a dilution of 1:1,000.

RPMI and DMEM were purchased from Sigma-Aldrich. FBS was obtained from Biowest. Recombinant human TGFβ1 was obtained from PeproTech. The inhibitors of the kinases of TGFβ receptors SB505124 and LY2109761 were purchased from Sigma-Aldrich and Cayman Chem, respectively. Protein G–Sepharose 4B conjugate was purchased from Invitrogen, Clarity western ECL Substrate was purchased from Bio-Rad Laboratories, complete protease inhibitor cocktail was purchased from Roche, and prestained protein molecular mass markers for SDS-PAGE were purchased from Thermo Fisher Scientific (PageRuler). DAPI fluorescent dye to visualize cell nuclei by microscopy was purchased from Merck.

Immunoblotting, immunoprecipitation, GST binding, and ubiquitination assays

Cell lysates were prepared in buffer containing 50 mM Tris-HCl, pH 7.4, 0.5% Triton X-100, 10 mM NaCl, 2 mM NaF, 2 mM sodium pyrophosphate, 2 mM β-glycerophosphate, 2 mM sodium orthovanadate, and protease inhibitors. The lysates were cleared by centrifugation at 13,000 rpm for 15 min at 4°C and protein concentrations were measured by Bradford assay (Bio-Rad Laboratories). For protein expression analysis, total cell lysates with adjusted protein concentration were separated by SDS-PAGE and transferred to nitrocellulose membranes, which were incubated with the indicated antibodies. Bound antibodies were visualized by enhanced chemiluminescence. For coimmunoprecipitation analysis, cell lysates were first cleared by incubation with protein G beads for 20 min, and then incubated with the indicated antibody for 2 h at 4°C before incubation with protein G beads for 1 h at 4°C. The beads were washed four times with ice-cold lysis buffer and twice with PBS, and immunocomplexes were eluted from the beads by adding 2× Laemmli SDS sample buffer and boiling for 5 min. Immunoblot analysis of the precipitated proteins was performed using indicated primary antibodies and corresponding anti–rabbit or anti–mouse IgG light chain–specific antibodies (1:10,000 dilution; Jackson ImmunoResearch Laboratories, Inc.). Immunoblots were analyzed by Quantity One software (Bio-Rad Laboratories).

For GST binding assays, GST fusion proteins were adsorbed on glutathione superflow agarose beads (Thermo Fisher Scientific), incubated with the lysates for 2 h at 4°C, and washed in the lysis buffer, and bound proteins were eluted and analyzed by Western blotting, as described in the previous paragraph. In vivo ubiquitination assay was performed, as previously described (Sorrentino et al., 2008). In brief, HEK293T cells were transfected as described in the figure legends, washed once in PBS, scraped in 1 ml PBS, and centrifuged at 400 *g* for 5 min. Non-covalent protein interactions were dissociated by boiling

for 5–10 min in 1% SDS. Samples were diluted in PBS (1:10) containing 0.5% NP-40 and cleared by centrifugation at 12,000 *g* for 10 min. The supernatants were subjected to immunoprecipitation with a CIN85 antibody, followed by immunoblotting with a ubiquitin antibody.

Cell migration assay

PC-3U cells were transfected with either empty pCDNA3 vector or Flag-CIN85 expression construct. At 48 h after transfection, transfected cells were selected by growing them in culture medium with 0.5 mg/ml G418 for 10 d. Cells were grown to confluence in 6-well plates (Sarstedt AG & Co.) and incubated for 16 h in medium with 0.1% FBS, and wounds were made using a pipette tip. 5 ng/ml TGFβ was added to the culture media immediately after wounding. Phase-contrast images were captured at indicated times and the imaging data were analyzed by the TScratch software (Gebäck et al., 2009). Motility of the cells was quantitated by 12 measurements in each experimental category and expressed as a percentage of the original open wound area.

TGFβ transcriptional activity analysis

Quantitative RT-PCR (qRT-PCR) analysis for expression of PAI-1 was performed on mRNA extracted from PC-3U cells transiently transfected with empty pCDNA3 (vector) or Flag-CIN85 and treated with TGFβ (5 ng/ml) for indicated time periods. Total cellular RNA was purified with the RNeasy mini kit (QIAGEN) and cDNA was synthesized from 0.5 µg RNA using the iQ SYBR Green supermix (Bio-Rad Laboratories). The results were normalized on the basis of GAPDH mRNA expression. The data were plotted as the mean fold induction of TGFβ-stimulated mRNA levels relative to unstimulated levels (0 h set to 1) with SDs determined from triplicate measurements. qRT-PCR conditions were as described previously (Mu et al., 2011) with primers used as follows: human CIN85 mRNA (SH3KBP1; GenBank accession no. NM_031892.2), 5′-TGCAGATGGAAGTGAACGAC-3′ (forward) and 5′-TGGGGCAGAAAATTTGAGTC-3′ (reverse); human PAI-1, 5′-CTCTCTCTGCCCTCACCAAC-3′ (forward) and 5′-GTGGAGAGGCTCTTGGTCTG-3′ (reverse); human GAPDH, 5′-GGAGTCAACGGATTTGGTCGTA-3′ (forward) and 5′-GGCAACAATATCCACTTTACCA-3′ (reverse).

The promoter-reporter assays were performed as previously described (Yakymovych et al., 2001). In brief, cells were transiently transfected with luciferase reporter vectors and pCMV-LacZ together with protein expression plasmids, as indicated in the figure legends. 24 h after transfection, the cells were starved for 20 h in culture medium with 1% FBS, and then stimulated with TGFβ for the next 24 h. The luciferase activity was analyzed with the Luciferase Assay System (Promega) using an EnSpire Multimode Plate Reader (PerkinElmer) and normalized on the basis of β-galactosidase activity. The data were plotted as mean values from triplicate determinations with SDs.

Biotinylation of cell surface TβRI and recycling assay

HEK293T cells or PC-3U were transfected with HA-TβRI in the absence or presence of Flag-tagged CIN85. 48 h after transfection, cells were starved in serum-low medium for 16 h and then treated with or without TGFβ (5 ng/ml) at 37°C. After indicated time periods, cells were washed with ice-cold PBS and incubated with 0.25 mg/ml sulfo-NHS-SS-biotin (Thermo Fisher Scientific) dissolved in PBS, supplemented with 0.9 mM $CaCl_2$ and 0.5 mM $MgCl_2$ (PBS^{2+}) for 30 min at 4°C. All unreacted biotin was removed by washing with 50 mM glycine and 0.5% BSA dissolved in PBS^{2+}, and cells were lysed in the RIPA buffer (50 mM Tris-HCl, pH 8, 150 mM NaCl, 1% NP-40, 0.5% sodium deoxycholate, 0.1% SDS, 25 mM NaF, 25 mM β-glycerophosphate, and protease inhibitors). Biotinylated proteins were precipitated with neutravidin-agarose beads (Thermo Fisher Scientific) and analyzed by immunoblotting using HA antibody. The levels of HA-TβRI and Flag-CIN85 expression were determined by immunoblotting of total cell lysates.

To study the effect of CIN85 overexpression on the TβRI recycling, we used biotinylation recycling assay according to Arancibia-Carcamo et al. (2006). Transfected COS7 cells were labeled with sulfo-NHS-SS-biotin at 4°C, as in the previous paragraph. Upon completion of biotin labeling, the culture media were changed and cells were incubated at 37°C for 60 min to resume membrane trafficking of the receptor. After the internalization step, all remaining surface sulfo-NHS-SS-biotin was stripped by extensive washing in 50 mM glutathione dissolved in 75 mM NaCl and 10 mM EDTA, pH 7.5, at 4°C. The cells were then incubated at 37°C for an additional 30 min in DMEM with 50 mM glutathione, pH 7.5. Control dishes were kept all the time at 4°C to prevent internalization and to monitor the efficacy of biotin stripping. The biotin of any sulfo-NHS-SS-biotinylated receptors that were recycled back to the cell surface was cleaved off by the glutathione present in the medium. At the end of incubation, biotinylated proteins were purified using streptavidin affinity chromatography and analyzed by immunoblotting. Immunoblots were analyzed by Quantity One software. In the lysates of the cells incubated with glutathione, all biotinylated HA-TβRI was internalized but not recycled during incubation, thus, inversely correlating with the rate of receptor recycling. The loss of biotinylated internalized receptors after the second biotin cleavage provides a measure of receptor recycling.

Subcellular fractionation

Subcellular fractionation was performed as described previously (Zhu et al., 2012). In short, the cells were washed with ice-cold PBS and homogenized in buffer (20 mM Hepes, pH 7.4, 1 mM EDTA, and 250 mM sucrose with protease and phosphatase inhibitors) 20 times with a 22-gauge needle and 5 times with a 26-gauge needle. The nuclei were pelleted at 3,000 *g* for 10 min at 4°C. After measurement of protein concentration, a 10–20–30% discontinuous gradient was generated by mixing postnuclear supernatant 1:1 with 60% iodixanol (OptiPrep; Sigma-Aldrich) and layered under 1.2 ml of 20% iodixanol with 1.2 ml of 10% iodixanol and 0.4 ml of homogenization buffer at the top of the centrifuge tubes. The samples were centrifuged at 260,000 *g* for 3 h at 4°C. Fractions (200–400 µl) were collected from the top of the gradient and equal volumes of each fraction were separated by electrophoresis in polyacrylamide gels and analyzed by immunoblotting for the presence of the endosomal markers (EEA1, Rab7, and Rab11) and HA-TβRI.

Lipid rafts were isolated using sucrose density centrifugation, as described by Ostrom and Insel (2006). In brief, HEK293T cells transfected with HA-TβRI alone or with Flag-CIN85 were grown to near confluence in 100-mm dishes. After two washes with ice-cold PBS, two confluent dishes were scraped into 1 ml of lysis buffer (1% Triton X-100, 25 mM 2-(*N*-morpholino) ethanesulfonic acid, 150 mM NaCl, and protease inhibitors, pH 6.0). Cells were homogenized by forcing lysates 10 times through a 25-gauge needle. The homogenates were adjusted to 45% sucrose, placed at the bottom of an ultracentrifuge tube, and overlaid with 35% and 5% sucrose. After centrifugation at 41,000 rpm for 24 h in a rotor (SW50.1; Beckman Coulter), 0.5-ml fractions were collected from the top of the tubes and a portion of each fraction was analyzed by SDS-PAGE.

Immunofluorescence assays

For all immunofluorescence studies, cells were seeded on sterile coverslips in 6-well plates, transfected, and treated, as indicated in figure legends. The coverslips were washed with PBS, fixed for 10 min in 4% paraformaldehyde, and permeabilized with 0.2% Triton X-100 in PBS for 5 min. Cells were blocked by 5% normal goat serum and incubated

with primary antibody in the antibody dilution buffer (1% BSA and 0.3% Triton X-100 in PBS). The proteins of interest were visualized by subsequent binding with Alexa Fluor–conjugated antibodies in the antibody dilution buffer. Control samples were labeled with the individual fluorophores and exposed identically as the dual-labeled samples at each wavelength to verify that there was no crossover among emission channels. After washing in PBS, coverslips were mounted with Fluoromount-G (SouthernBiotech) mounting medium. Standard fluorescence microscopy digital images were acquired at room temperature using an oil immersion 60× objective (numerical aperture 1.40) on a fluorescence microscope (Axio Imager.M2; Carl Zeiss) equipped with a Retiga EXi camera (QImaging) and controlled by ZEN software (Carl Zeiss). Acquired images were processed and analyzed using ImageJ software (National Institutes of Health).

Histology of human prostate cancer tissues

Tissue sections of normal and malignant tissues were provided by Umeå University Hospital and ethical permit was granted by the Umeå ethical review board in full agreement with the Swedish Ethical Review Act (540/03, Dnr 03-482).

For immunohistochemistry staining the sections were rehydrated in xylene two times each for 10 min, 100% ethanol for 10 min, and 95%, 80%, and 70% ethanol and deionized H_2O each for 5 min. Then the sections were treated with Antigen Retrieval Reagent (R&D systems) at 95°C for 5 min, rinsed with PBS, kept in 3% H_2O_2/100% methanol for 10 min, washed twice with PBS, blocked in 5% normal goat serum for 1 h at room temperature, and incubated with primary antibodies CIN85 (1:100; Sigma-Aldrich) overnight at 4°C. After washing with PBS three times each for 5 min, the sections were incubated with secondary antibody (DAKO) for 45 min at room temperature followed by three washes in PBS. Then, the sections were developed with AEC (Vector Laboratories), counterstained with hematoxylin, and mounted in aqueous mounting medium (Vector Laboratories).

For immunohistofluorescence staining, the sections were deparaffinized and retrieved in the same way as described in the previous paragraph. After blocking in 1% horse serum in PBS for 1 h at room temperature, the sections were incubated with primary antibodies (CIN85 [Sigma-Aldrich] diluted 1:50 and phospho-Smad2 diluted 1:50) overnight at 4°C. After washing in PBS three times each for 5 min, the sections were incubated with NorthernLights secondary antibody (R&D Systems) for 45 min at room temperature. Finally, the sections were washed with PBS three times each for 5 min, and thereafter mounted with mounting medium with DAPI (Vector Laboratories).

Digital images of stainings were acquired by scanning with Pannoramic 250 Flash II (3DHistech) or a fluorescence microscope (Axioplan 2; Carl Zeiss, and analyzed by ImageJ software. Grayscale values (pixel intensities) were measured and calculated to compare the intensity of different stainings. Means ± SEM were obtained from different groups, and Students' *t* tests were used to evaluate the differences between the groups compared.

Online supplemental material

Fig. S1 provides evidence that interaction between TβRI and CIN85 is not altered by TGFβ receptors kinase inhibitors, dynamin inhibitor, or low temperature. Fig. S2 shows that HA-TβRI interacts with the SH3 domains of CIN85 in a GST pull-down assay and that in vitro ubiquitination of GST-TβRI increases the amount of CIN85 precipitated in a GST pull-down assay; overexpression of TRAF6 has no effect on the interaction between TβRII and CIN85. Fig. S3 shows that overexpression of CIN85 alters TβRI distribution in an iodixanol density gradient membrane flotation assay, but does not change the localization of TβRI to lipid rafts. Fig. S4 provides evidence that overexpression of CIN85 increases the recycling rate of HA-TβRI in COS7 cells. Fig. S5 demonstrates that CIN85 expression correlates with higher level of phosphorylated Smad2 in prostate cancer tissue. Online supplemental material is available at http://www.jcb.org/cgi/content/full/jcb.201411025/DC1.

Acknowledgments

We thank Pernilla Andersson for skillful technical assistance with human prostate tissue samples, Dr. Wanzhong Wang for expert histopathological evaluation of prostate cancer tissues, and Dr. Nikolay Aksenov for selection of CIN85 primers used in qRT-PCR.

This work was supported by the Ludwig Institute for Cancer Research and grants to M. Landström from the Knut and Alice Wallenberg Foundation (2012.0090), Swedish Medical Research Council (K2013-66X-15284-04-4), and the Swedish Cancer Society (13 0688).

The authors declare no competing financial interests.

Submitted: 7 November 2014
Accepted: 3 June 2015

References

Aissouni, Y., G. Zapart, J.L. Iovanna, I. Dikic, and P. Soubeyran. 2005. CIN85 regulates the ability of MEKK4 to activate the p38 MAP kinase pathway. *Biochem. Biophys. Res. Commun.* 338:808–814. http://dx.doi.org/10.1016/j.bbrc.2005.10.032

Arancibia-Carcamo, I.L., B.P. Fairfax, S.J. Moss, and J.T. Kittler. 2006. Studying the localization, surface stability and endocytosis of neurotransmitter receptors by antibody labeling and biotinylation approaches. *In* The Dynamic Synapse: Molecular Methods in Ionotropic Receptor Biology. J.T. Kittler and S.J. Moss, editors. CRC Press, Boca Raton, FL. 91–118.

Bezsonova, I., M.C. Bruce, S. Wiesner, H. Lin, D. Rotin, and J.D. Forman-Kay. 2008. Interactions between the three CIN85 SH3 domains and ubiquitin: implications for CIN85 ubiquitination. *Biochemistry.* 47:8937–8949. http://dx.doi.org/10.1021/bi800439t

Chen, Y.G. 2009. Endocytic regulation of TGF-β signaling. *Cell Res.* 19:58–70. http://dx.doi.org/10.1038/cr.2008.315

Chen, X., M.J. Rubock, and M. Whitman. 1996. A transcriptional partner for MAD proteins in TGF-β signalling. *Nature.* 383:691–696. http://dx.doi.org/10.1038/383691a0

Dennler, S., S. Itoh, D. Vivien, P. ten Dijke, S. Huet, and J.-M. Gauthier. 1998. Direct binding of Smad3 and Smad4 to critical TGFβ-inducible elements in the promoter of human plasminogen activator inhibitor-type 1 gene. *EMBO J.* 17:3091–3100. http://dx.doi.org/10.1093/emboj/17.11.3091

Di Guglielmo, G.M., C. Le Roy, A.F. Goodfellow, and J.L. Wrana. 2003. Distinct endocytic pathways regulate TGF-β receptor signalling and turnover. *Nat. Cell Biol.* 5:410–421. http://dx.doi.org/10.1038/ncb975

Dikic, I. 2002. CIN85/CMS family of adaptor molecules. *FEBS Lett.* 529:110–115. http://dx.doi.org/10.1016/S0014-5793(02)03188-5

Franzén, P., H. Ichijo, and K. Miyazono. 1993. Different signals mediate transforming growth factor-β1-induced growth inhibition and extracellular matrix production in prostatic carcinoma cells. *Exp. Cell Res.* 207:1–7. http://dx.doi.org/10.1006/excr.1993.1156

Gebäck, T., M.M. Schulz, P. Koumoutsakos, and M. Detmar. 2009. TScratch: a novel and simple software tool for automated analysis of monolayer wound healing assays. *Biotechniques.* 46:265–274.

Gleason, R.J., A.M. Akintobi, B.D. Grant, and R.W. Padgett. 2014. BMP signaling requires retromer-dependent recycling of the type I receptor. *Proc. Natl. Acad. Sci. USA.* 111:2578–2583. http://dx.doi.org/10.1073/pnas.1319947111

Gout, I., G. Middleton, J. Adu, N.N. Ninkina, L.B. Drobot, V. Filonenko, G. Matsuka, A.M. Davies, M. Waterfield, and V.L. Buchman. 2000. Negative regulation of PI 3-kinase by Ruk, a novel adaptor protein. *EMBO J.* 19:4015–4025. http://dx.doi.org/10.1093/emboj/19.15.4015

Havrylov, S., M.J. Redowicz, and V.L. Buchman. 2010. Emerging roles of Ruk/CIN85 in vesicle-mediated transport, adhesion, migration and malignancy. *Traffic.* 11:721–731. http://dx.doi.org/10.1111/j.1600-0854.2010.01061.x

Heldin, C.-H., and A. Moustakas. 2012. Role of Smads in TGFβ signaling. *Cell Tissue Res.* 347:21–36. http://dx.doi.org/10.1007/s00441-011-1190-x

Kardassis, D., C. Murphy, T. Fotsis, A. Moustakas, and C. Stournaras. 2009. Control of transforming growth factor β signal transduction by small GTPases. *FEBS J.* 276:2947–2965. http://dx.doi.org/10.1111/j.1742-4658.2009.07031.x

Karlsson, S., K. Kowanetz, A. Sandin, C. Persson, A. Ostman, C.H. Heldin, and C. Hellberg. 2006. Loss of T-cell protein tyrosine phosphatase induces recycling of the platelet-derived growth factor (PDGF) β-receptor but not the PDGF α-receptor. *Mol. Biol. Cell.* 17:4846–4855. http://dx.doi.org/10.1091/mbc.E06-04-0306

Kim, J., D. Kang, B.K. Sun, J.-H. Kim, and J.J. Song. 2013. TRAIL/MEKK4/p38/HSP27/Akt survival network is biphasically modulated by the Src/CIN85/c-Cbl complex. *Cell. Signal.* 25:372–379. http://dx.doi.org/10.1016/j.cellsig.2012.10.010

Kometani, K., T. Yamada, Y. Sasaki, T. Yokosuka, T. Saito, K. Rajewsky, M. Ishiai, M. Hikida, and T. Kurosaki. 2011. CIN85 drives B cell responses by linking BCR signals to the canonical NF-κB pathway. *J. Exp. Med.* 208:1447–1457. http://dx.doi.org/10.1084/jem.20102665

Kowanetz, K., J. Terzic, and I. Dikic. 2003. Dab2 links CIN85 with clathrin-mediated receptor internalization. *FEBS Lett.* 554:81–87. http://dx.doi.org/10.1016/S0014-5793(03)01111-6

Kowanetz, K., K. Husnjak, D. Höller, M. Kowanetz, P. Soubeyran, D. Hirsch, M.H.H. Schmidt, K. Pavelic, P. De Camilli, P.A. Randazzo, and I. Dikic. 2004. CIN85 associates with multiple effectors controlling intracellular trafficking of epidermal growth factor receptors. *Mol. Biol. Cell.* 15:3155–3166. http://dx.doi.org/10.1091/mbc.E03-09-0683

Lin, H.-K., S. Bergmann, and P.P. Pandolfi. 2004. Cytoplasmic PML function in TGF-β signalling. *Nature.* 431:205–211. http://dx.doi.org/10.1038/nature02783

Lynch, D.K., S.C. Winata, R.J. Lyons, W.E. Hughes, G.M. Lehrbach, V. Wasinger, G. Corthals, S. Cordwell, and R.J. Daly. 2003. A Cortactin-CD2-associated protein (CD2AP) complex provides a novel link between epidermal growth factor receptor endocytosis and the actin cytoskeleton. *J. Biol. Chem.* 278:21805–21813. http://dx.doi.org/10.1074/jbc.M211407200

Massagué, J. 2008. TGFβ in cancer. *Cell.* 134:215–230. http://dx.doi.org/10.1016/j.cell.2008.07.001

Mishra, L., and B. Marshall. 2006. Adaptor proteins and ubiquinators in TGF-β signaling. *Cytokine Growth Factor Rev.* 17:75–87. http://dx.doi.org/10.1016/j.cytogfr.2005.09.001

Mitchell, H., A. Choudhury, R.E. Pagano, and E.B. Leof. 2004. Ligand-dependent and -independent transforming growth factor-β receptor recycling regulated by clathrin-mediated endocytosis and Rab11. *Mol. Biol. Cell.* 15:4166–4178. http://dx.doi.org/10.1091/mbc.E04-03-0245

Mu, Y., R. Sundar, N. Thakur, M. Ekman, S.K. Gudey, M. Yakymovych, A. Hermansson, H. Dimitriou, M.T. Bengoechea-Alonso, J. Ericsson, et al. 2011. TRAF6 ubiquitinates TGFβ type I receptor to promote its cleavage and nuclear translocation in cancer. *Nat. Commun.* 2:330. http://dx.doi.org/10.1038/ncomms1332

Mu, Y., S.K. Gudey, and M. Landström. 2012. Non-Smad signaling pathways. *Cell Tissue Res.* 347:11–20. http://dx.doi.org/10.1007/s00441-011-1201-y

Narita, T., T. Nishimura, K. Yoshizaki, and T. Taniyama. 2005. CIN85 associates with TNF receptor 1 via Src and modulates TNF-α-induced apoptosis. *Exp. Cell Res.* 304:256–264. http://dx.doi.org/10.1016/j.yexcr.2004.11.005

Ostrom, R.S., and P.A. Insel. 2006. Methods for the study of signaling molecules in membrane lipid rafts and caveolae. *Methods Mol. Biol.* 332:181–191.

Penheiter, S.G., R.D. Singh, C.E. Repellin, M.C. Wilkes, M. Edens, P.H. Howe, R.E. Pagano, and E.B. Leof. 2010. Type II transforming growth factor-β receptor recycling is dependent upon the clathrin adaptor protein Dab2. *Mol. Biol. Cell.* 21:4009–4019. http://dx.doi.org/10.1091/mbc.E09-12-1019

Persson, U., H. Izumi, S. Souchelnytskyi, S. Itoh, S. Grimsby, U. Engström, C.H. Heldin, K. Funa, and P. ten Dijke. 1998. The L45 loop in type I receptors for TGF-β family members is a critical determinant in specifying Smad isoform activation. *FEBS Lett.* 434:83–87. http://dx.doi.org/10.1016/S0014-5793(98)00954-5

Peruzzi, G., R. Molfetta, F. Gasparrini, L. Vian, S. Morrone, M. Piccoli, L. Frati, A. Santoni, and R. Paolini. 2007. The adaptor molecule CIN85 regulates Syk tyrosine kinase level by activating the ubiquitin-proteasome degradation pathway. *J. Immunol.* 179:2089–2096. http://dx.doi.org/10.4049/jimmunol.179.4.2089

Petrelli, A., G.F. Gilestro, S. Lanzardo, P.M. Comoglio, N. Migone, and S. Giordano. 2002. The endophilin–CIN85–Cbl complex mediates ligand-dependent downregulation of c-Met. *Nature.* 416:187–190. http://dx.doi.org/10.1038/416187a

Rønning, S.B., N.M. Pedersen, I.H. Madshus, and E. Stang. 2011. CIN85 regulates ubiquitination and degradative endosomal sorting of the EGF receptor. *Exp. Cell Res.* 317:1804–1816. http://dx.doi.org/10.1016/j.yexcr.2011.05.016

Schroeder, B., S.G. Weller, J. Chen, D. Billadeau, and M.A. McNiven. 2010. A Dyn2-CIN85 complex mediates degradative traffic of the EGFR by regulation of late endosomal budding. *EMBO J.* 29:3039–3053. http://dx.doi.org/10.1038/emboj.2010.190

Schroeder, B., S. Srivatsan, A. Shaw, D. Billadeau, and M.A. McNiven. 2012. CIN85 phosphorylation is essential for EGFR ubiquitination and sorting into multivesicular bodies. *Mol. Biol. Cell.* 23:3602–3611. http://dx.doi.org/10.1091/mbc.E11-08-0666

Shimokawa, N., K. Haglund, S.M. Hölter, C. Grabbe, V. Kirkin, N. Koibuchi, C. Schultz, J. Rozman, D. Hoeller, C.-H. Qiu, et al. 2010. CIN85 regulates dopamine receptor endocytosis and governs behaviour in mice. *EMBO J.* 29:2421–2432. http://dx.doi.org/10.1038/emboj.2010.120

Sorrentino, A., N. Thakur, S. Grimsby, A. Marcusson, V. von Bulow, N. Schuster, S. Zhang, C.-H. Heldin, and M. Landström. 2008. The type I TGF-β receptor engages TRAF6 to activate TAK1 in a receptor kinase-independent manner. *Nat. Cell Biol.* 10:1199–1207. http://dx.doi.org/10.1038/ncb1780

Soubeyran, P., K. Kowanetz, I. Szymkiewicz, W.Y. Langdon, and I. Dikic. 2002. Cbl–CIN85–endophilin complex mediates ligand-induced downregulation of EGF receptors. *Nature.* 416:183–187. http://dx.doi.org/10.1038/416183a

Sundar, R., S.K. Gudey, C.H. Heldin, and M. Landström. 2015. TRAF6 promotes TGFβ-induced invasion and cell-cycle regulation via Lys63-linked polyubiquitination of Lys178 in TGFβ type I receptor. *Cell Cycle.* 14:554–565. http://dx.doi.org/10.4161/15384101.2014.990302

Szymkiewicz, I., K. Kowanetz, P. Soubeyran, A. Dinarina, S. Lipkowitz, and I. Dikic. 2002. CIN85 participates in Cbl-b-mediated down-regulation of receptor tyrosine kinases. *J. Biol. Chem.* 277:39666–39672. http://dx.doi.org/10.1074/jbc.M205535200

Szymkiewicz, I., O. Shupliakov, and I. Dikic. 2004. Cargo- and compartment-selective endocytic scaffold proteins. *Biochem. J.* 383:1–11. http://dx.doi.org/10.1042/BJ20040913

Thompson, T.C., L.D. Truong, T.L. Timme, D. Kadmon, B.K. McCune, K.C. Flanders, P.T. Scardino, and S.H. Park. 1992. Transforming growth factor β1 as a biomarker for prostate cancer. *J. Cell. Biochem. Suppl.* 16H:54–61. http://dx.doi.org/10.1002/jcb.240501212

Watanabe, S., H. Take, K. Takeda, Z.X. Yu, N. Iwata, and S. Kajigaya. 2000. Characterization of the CIN85 adaptor protein and identification of components involved in CIN85 complexes. *Biochem. Biophys. Res. Commun.* 278:167–174. http://dx.doi.org/10.1006/bbrc.2000.3760

Xu, P., J. Liu, and R. Derynck. 2012. Post-translational regulation of TGF-β receptor and Smad signaling. *FEBS Lett.* 586:1871–1884. http://dx.doi.org/10.1016/j.febslet.2012.05.010

Yakymovych, I., P. Ten Dijke, C.-H. Heldin, and S. Souchelnytskyi. 2001. Regulation of Smad signaling by protein kinase C. *FASEB J.* 15:553–555.

Yamashita, M., K. Fatyol, C. Jin, X. Wang, Z. Liu, and Y.E. Zhang. 2008. TRAF6 mediates Smad-independent activation of JNK and p38 by TGF-β. *Mol. Cell.* 31:918–924. http://dx.doi.org/10.1016/j.molcel.2008.09.002

Zhang, J., X. Zheng, X. Yang, and K. Liao. 2009. CIN85 associates with endosomal membrane and binds phosphatidic acid. *Cell Res.* 19:733–746. http://dx.doi.org/10.1038/cr.2009.51

Zhu, L., L. Wang, X. Luo, Y. Zhang, Q. Ding, X. Jiang, X. Wang, Y. Pan, and Y. Chen. 2012. Tollip, an intracellular trafficking protein, is a novel modulator of the transforming growth factor-β signaling pathway. *J. Biol. Chem.* 287:39653–39663. http://dx.doi.org/10.1074/jbc.M112.388009